Electroweak baryogenesis in two Higgs doublet model with alignment scenario

Yushi Mura (Osaka Univ.)

Collaborators: Kazuki Enomoto (KAIST), Shinya Kanemura (Osaka Univ.)

2023/06/07

Higgs as a Probe of New Physics 2023 in Osaka

Based on

K. Enomoto, S. Kanemura, and Y.M, JHEP 01 (2022) 104, arXiv: 2111.13079 [hep-ph],

K. Enomoto, S. Kanemura, and Y.M, JHEP 09 (2022) 121, arXiv: 2207.00060 [hep-ph],

S. Kanemura, and Y.M, arXiv: 2303.11252 [hep-ph]

Introduction

- **SM cannot explain Baryon Asymmetry of the Universe**

  From Cosmological observation, $\eta_B^{obs} = \frac{n_B - n_{\bar{B}}}{s} \simeq 8.7 \times 10^{-11}$ PDG (2022)

- **Baryogenesis in the early Universe**

  Sakharov conditions Sakharov (1967)
  ① Baryon number violation
  ② C and CP violation
  ③ Departure from thermal equilibrium

- **Well motivated scenario**

  Electroweak Baryogenesis Kuzmin, Rubakov and Shaposhnikov (1985)
  ① Sphaleron process
  ② Electroweak theory with CP violation
  ③ First order electroweak phase transition

Electroweak Baryogenesis

- **Expanding bubble walls created at first order PT**

- **Sphaleron process must be decoupled inside the bubble**

$$\Gamma_{sph}^{brk}(T_n) < H(T_n) \Longrightarrow v_n/T_n \gtrsim 1$$ →Strongly first order PT

In the SM, however,

- Cross over phase transition
- Insufficient CP violation

Huet and Sather (1995)
Kajantie *et al.* (1996)

Extended Higgs sectors are needed

Ex) Two Higgs Doublet Model : SM + Higgs doublet

Fromme, Huber and Seniuchi (2006); Cline, Kainulainen and Trott (2011); and more

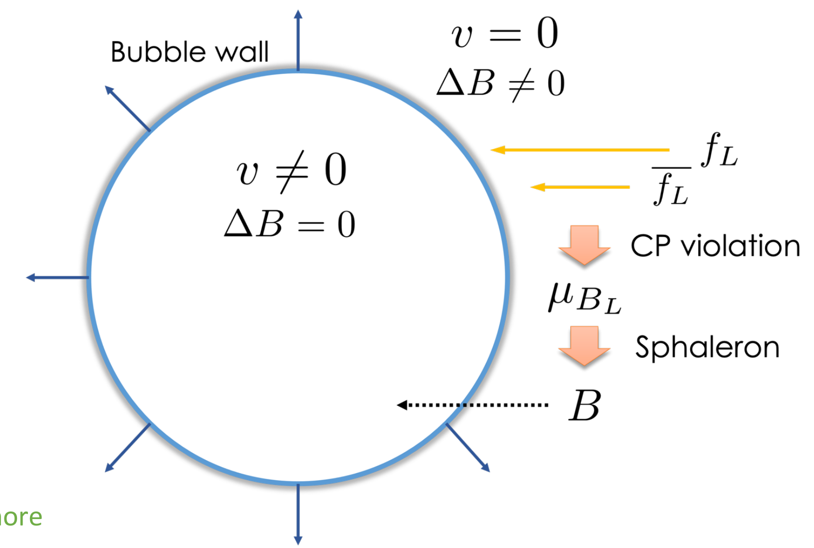

- **Experimental constraints**

  - Higgs alignment supported by LHC ATLAS, Nature (2022); CMS, CMS-PAS-HIG-19-005 (2020)
  - Measurements of electric dipole moment for additional CP violation Andreev *et al.* [ACME] (2018) Roussy *et al.* [Cornell Group] (2022)

Aligned Two Higgs Doublet Model

- **Most general two Higgs doublet model** $\Phi_1 = \begin{pmatrix} G^+ \\ \frac{1}{\sqrt{2}}(v + h_1 + iG^0) \end{pmatrix}, \quad \Phi_2 = \begin{pmatrix} H^+ \\ \frac{1}{\sqrt{2}}(h_2 + ih_3) \end{pmatrix}$

$$
\begin{aligned}
V =& -\mu_1{}^2(\Phi_1{}^\dagger\Phi_1) - \mu_2{}^2(\Phi_2{}^\dagger\Phi_2) - \left(\mu_3{}^2(\Phi_1{}^\dagger\Phi_2) + h.c.\right) \\
&+ \frac{1}{2}\lambda_1(\Phi_1{}^\dagger\Phi_1)^2 + \frac{1}{2}\lambda_2(\Phi_2{}^\dagger\Phi_2)^2 + \lambda_3(\Phi_1{}^\dagger\Phi_1)(\Phi_2{}^\dagger\Phi_2) + \lambda_4(\Phi_2{}^\dagger\Phi_1)(\Phi_1{}^\dagger\Phi_2) \\
&+ \left\{\left(\frac{1}{2}\lambda_5\Phi_1{}^\dagger\Phi_2 + \lambda_6\Phi_1{}^\dagger\Phi_1 + \lambda_7\Phi_2{}^\dagger\Phi_2\right)\Phi_1{}^\dagger\Phi_2 + h.c.\right\}, \quad (\mu_3, \lambda_5, \lambda_6, \lambda_7 \in \mathbb{C})
\end{aligned}
$$

Higgs basis
Davidson and Haber (2005)

Charged scalar $m_{H^\pm}^2 = M^2 + \frac{1}{2}\lambda_3 v^2 \qquad M^2 \equiv -\mu_2^2$

Neutral scalars
$$
\mathcal{M}^2 = v^2 \begin{pmatrix} \lambda_1 & \mathrm{Re}\lambda_6 & -\mathrm{Im}\lambda_6 \\ \mathrm{Re}\lambda_6 & \frac{M^2}{v^2} + \frac{\lambda_3+\lambda_4+\mathrm{Re}\lambda_5}{2} & \cancel{-\frac{1}{2}\mathrm{Im}\lambda_5} \\ -\mathrm{Im}\lambda_6 & \cancel{-\frac{1}{2}\mathrm{Im}\lambda_5} & \frac{M^2}{v^2} + \frac{\lambda_3+\lambda_4-\mathrm{Re}\lambda_5}{2} \end{pmatrix}
$$

"Mixing angle among neutral scalars are small" ⇒ consider $\lambda_6 = 0$ region

$$
= \begin{pmatrix} m_h^2 & 0 & 0 \\ 0 & m_{H_2}^2 & 0 \\ 0 & 0 & m_{H_3}^2 \end{pmatrix}
$$

Higgs alignment

- **Only** $\arg[\lambda_7] \equiv \theta_7$ **remains in the potential**

Most general Yukawa interaction

- **General structure of Yukawa interaction**

h SM Higgs

$H_{2,3}$ Additional scalars

up-type quark

$$-\mathcal{L}_Y = \overline{u_{i,L}} \frac{y_i \delta_{ij}}{\sqrt{2}} u_{j,R} h - \overline{u_{i,L}} \frac{\rho_{ij}}{\sqrt{2}} u_{j,R} H_2 - \overline{u_{i,L}} \frac{i\rho_{ij}}{\sqrt{2}} u_{j,R} H_3 + \mathrm{h.c.}$$

- **Small FCNC couplings related to the heavy scalars**

- **Top-charm sector can be sizable under current data.**

Ex) $\rho_{tc} \lesssim O(1)$

- **Consider two cases**

Top transport scenario

$$\rho^u = \zeta_u^* \,\mathrm{diag}(y_u, y_c, y_t), \quad \rho^d = \zeta_d \,\mathrm{diag}(y_d, y_s, y_b), \quad \rho^e = \zeta_e \,\mathrm{diag}(y_e, y_\mu, y_\tau),$$

Pich and Tuzon (2009)

Top-charm transport scenario

$$\rho^u = \begin{pmatrix} 0 & 0 & 0 \\ 0 & \rho_{cc} & \rho_{ct} \\ 0 & \rho_{tc} & \rho_{tt} \end{pmatrix}, \qquad \rho^d = \begin{cases} \rho_{bb} \ (i = j = 3) \\ 0 \quad (\text{others}) \end{cases} \qquad \text{and} \qquad \rho^e = 0$$

Summary of the model

- **Alignment scenario**

  One SM like Higgs and three additional scalars

- **CP violating parameters**

  Potential $\arg[\lambda_7] \equiv \theta_7$

  Yukawa

  Top transport $\arg[\zeta_u] \equiv \theta_u\,,\ \arg[\zeta_d] \equiv \theta_d,\ \arg[\zeta_e] \equiv \theta_e$

  Top-charm transport $\arg\left[\rho^u_{ij}\right] \equiv \theta_{ij}\,,\ \ \arg[\rho_{bb}] \equiv \theta_{bb}$

- **Electron EDM constraint**

  $|d_e| < 4.1{\times}10^{-30}\ e$ cm

  Roussy *et al.* [Cornell Group] arXiv:2212.11841

$d_e \simeq$

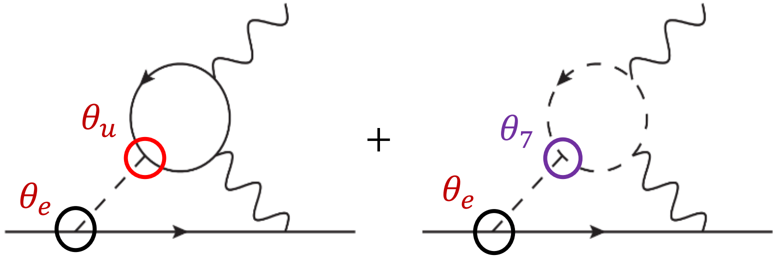

(a) Fermion-loop. (b) Higgs boson-loop.

- **Other experimental and theoretical constraints**

  Direct detection, EW precision, EDMs,
  perturbative unitarity, vacuum stability and triviality bound

Top transport scenario

$M = 30\,\mathrm{GeV},\ \lambda_2 = 0.1,\ |\lambda_7| = 0.8,\ \theta_7 = -0.9,$
$|\zeta_u| = |\zeta_d| = |\zeta_e| = 0.18,\ \theta_u = \theta_d = -2.7,\ \theta_e = -2.66.$

- **Benchmark points**

  ▼ BP1: strong PT $v_n/T_n = 2.4$
  ◆ BP2: weak PT $v_n/T_n = 2.0$

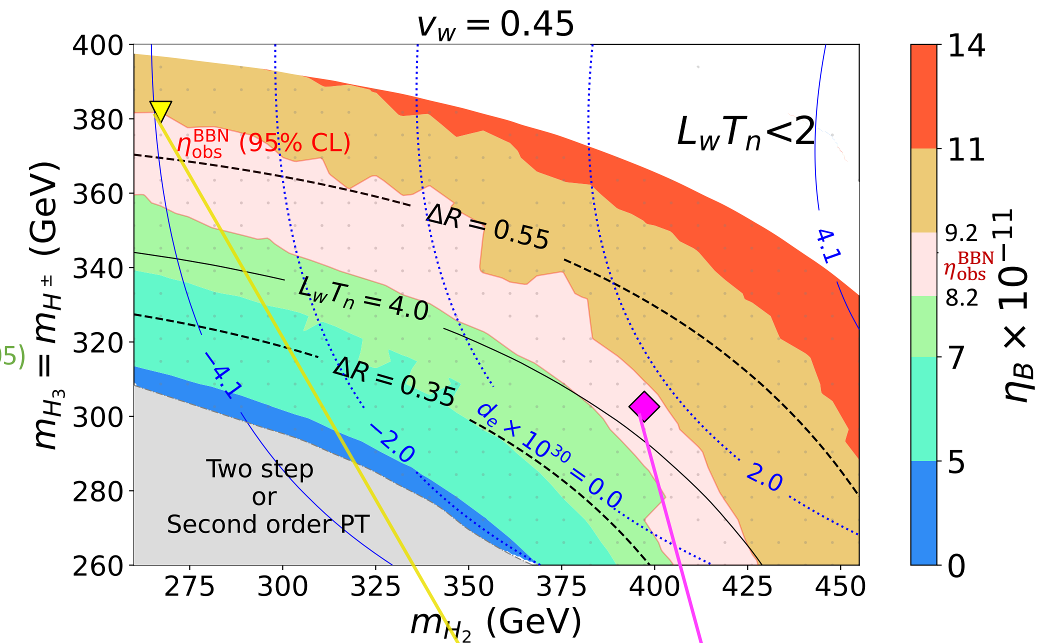

- **Triple Higgs coupling**

Kanemura, Okada and Senaha (2005)

$$m_\Phi^2 = M^2 + \tilde{\lambda} v^2 \simeq \tilde{\lambda} v^2$$

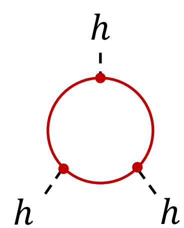

▼ BP1 $\Delta R = 61\%$
◆ BP2 $\Delta R = 44\%$

$(\Delta R \equiv \delta\lambda_{hhh}/\lambda_{hhh}^{\rm SM})$

Capeda *et al.* CERN Yellow Rep. Monogr. 7 (2019);
Fujii *et al.* [1506.05992]; Bambade *et al.* [1903.01629]
de Blas *et al.* [1812.02093]

HL-LHC : 50%
ILC 500GeV (1TeV) : 27% (10%)
CLIC 1.4TeV (3TeV) : ~30% (~10%)

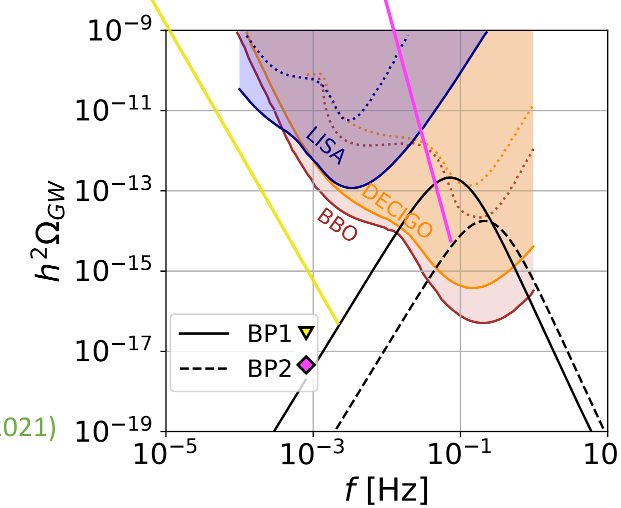

- **Gravitational waves**

Grojean and Servant (2007);
Kakizaki, Kanemura and Matsui (2015); and more

Peak integrated sensitivity curves Breitbach *et al.* (2019); Cline *et al.* (2021)

Future observations : LISA, DECIGO, BBO

Top-charm transport scenario

- **Benchmark point (wall velocity = 0.1)**

Related to…

phase transition and BAU

$$m_\Phi \equiv m_{H_2} = m_{H_3} = m_{H^\pm} = 350\ \mathrm{GeV},\ M = 20\ \mathrm{GeV},$$
$$\lambda_2 = 0.01,\ |\lambda_7| = 1.0,\ \arg(\lambda_7) = -2.4,\ |\rho_{tt}| = 0.1,\ \theta_{tt} = -0.2,$$

constraints and predictions

$$|\rho_{cc}| = 0.09,\ |\rho_{ct}| = 0.05,\ \theta_{cc} = 0,\ \theta_{ct} = -2.8,\ \theta_{tc} = -0.2,$$
$$|\rho_{bb}| = 1.0 \times 10^{-3},\ \theta_{bb} = 1.5.$$

- **$|\rho_{tc}|$ contributes to the BAU by picking up the effect of θ_7**

magenta : observed BAU $\eta_B = 8.7\times10^{-11}$

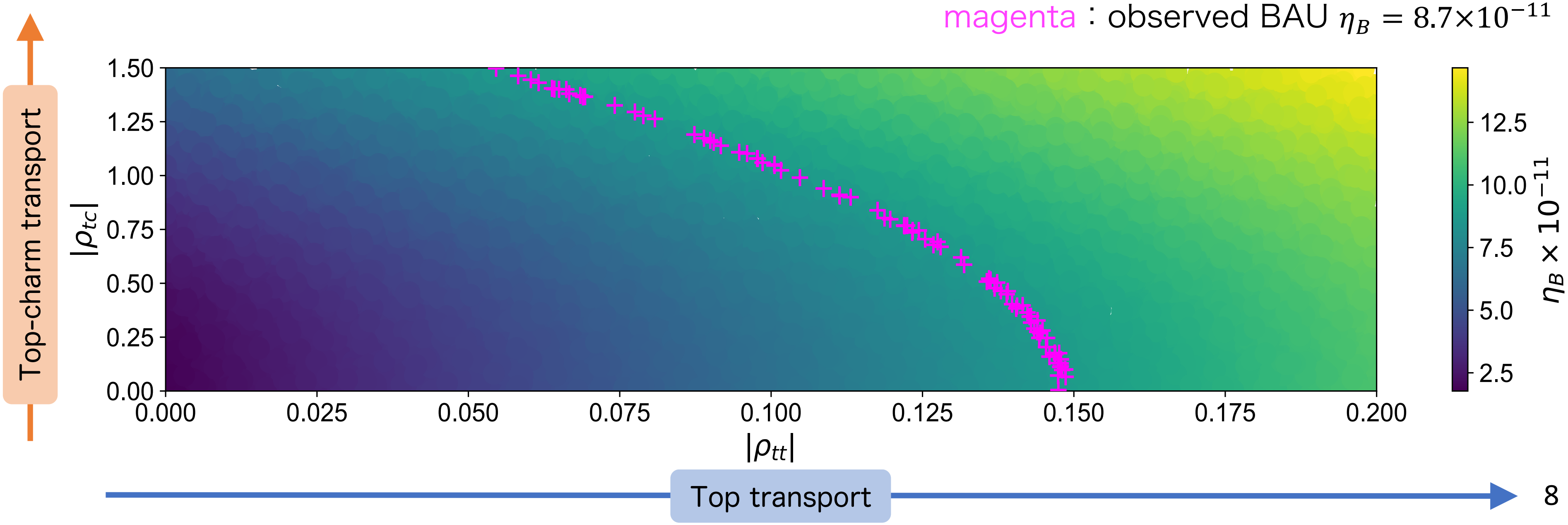

Top-charm transport scenario

- **Flavor constraints on FCNC couplings**

Green : $B_s \to \mu\mu$ CMS (2022)
Gray : ϵ_K ($K^0 - \overline{K^0}$ mixing) Chen and Nomur (2018)

Others : $B_d - \overline{B_d}$, $B_s - \overline{B_s}$ mixing and $B \to X_s\gamma$
UTfit (2018), J. Haller et.al. (2018) and HFLAV (2022)

- **Predictions for future Kaon physics**

Blue : $\Delta R_\nu^+ = \mathrm{Br}(K^+ \to \pi^+\nu\bar{\nu})/\mathrm{Br}(K^+ \to \pi^+\nu\bar{\nu})_{\mathrm{SM}} - 1$ [%]
Orange : $\Delta R_\nu^0 = \mathrm{Br}(K_L \to \pi^0\nu\bar{\nu})/\mathrm{Br}(K_L \to \pi^0\nu\bar{\nu})_{\mathrm{SM}} - 1$ [%]
Black : $(\epsilon'/\epsilon)_{\mathrm{2HDM}} \times 10^4$

Iguro and Omura (2019)
Hou and Kumar (2022)

magenta : observed BAU $\eta_B = 8.7\times10^{-11}$

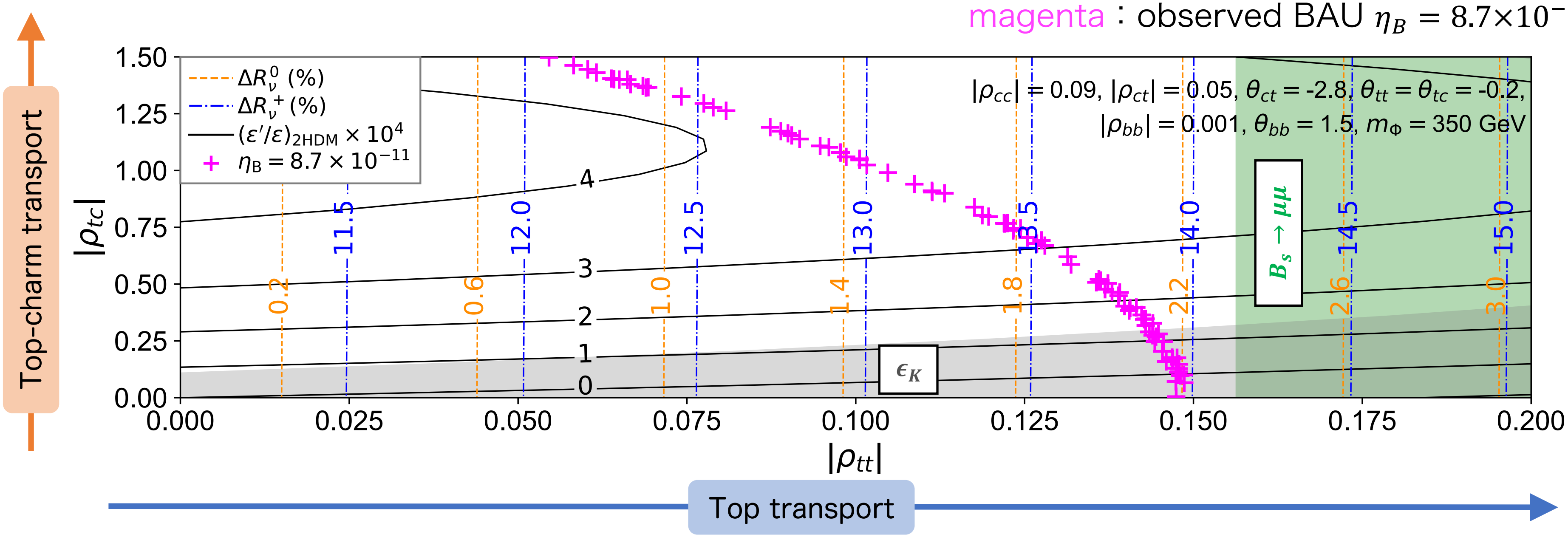

Summary

◆ **SM cannot explain the Baryon Asymmetry of the Universe**

EWBG as a solution of the BAU is well motivated scenario.

◆ **Two Higgs Doublet Model with alignment scenario**

- SM like Higgs boson
- Multiple CP phases in the model
- Which CPV interactions are important for the BAU ?

◆ **Phenomenology**

- Common testability
  - Higgs self coupling (ILC, CLIC, HL-LHC)
  - Gravitational waves (LISA, DECIGO, BBO)
  - EDM, Direct detection and Flavor experiments
- Top-charm transport scenario → Kaon physics becomes important.

Back up slides

About top-charm

Source term with top-charm mixing

- Two flavor fermions system

$$\mathcal{L}_{\rm mass} = -\overline{q_L} M(z) q_R + {\rm h.c.}, \quad q = (c, t)^T$$

$$M(z) = \frac{1}{\sqrt{2}} \begin{pmatrix} y_c\varphi_1 + \rho_{cc}(\varphi_2 - i\varphi_3) & \rho_{ct}(\varphi_2 - i\varphi_3) \\ \rho_{tc}(\varphi_2 - i\varphi_3) & y_t\varphi_1 + \rho_{tt}(\varphi_2 - i\varphi_3) \end{pmatrix}$$

φ_1: Real part of $\langle \Phi_1^0 \rangle$, φ_2: Real part of $\langle \Phi_2^0 \rangle$,
φ_3: Imaginary part of $\langle \Phi_2^0 \rangle$,

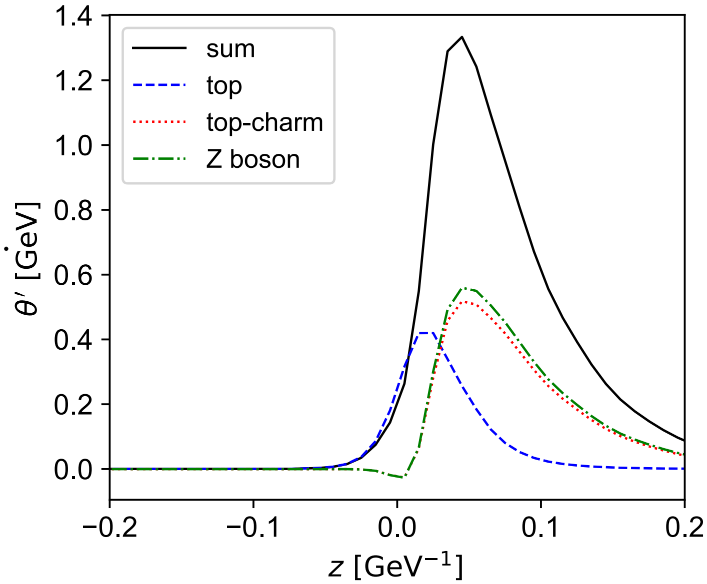

- WKB method

Cline, Joyce and Kainulainen, JHEP 07 (2000);
Cline and Kainulainen, Phys. Rev. D 101 (2020)

- ${\rm Abs}[\rho_{tc}]$ contributes to source term picking up CPV phase of the potential.

$$\theta' = \frac{1}{2m_+^2} \left\{ (|\rho_{tc}|^2 + |\rho_{tt}|^2)(\varphi_3\varphi_2' - \varphi_2\varphi_3') + y_t|\rho_{tt}| \Big((\varphi_3\varphi_1' - \varphi_1\varphi_3') \cos\theta_{tt} + (\varphi_1\varphi_2' - \varphi_2\varphi_1') \sin\theta_{tt} \Big) \right\}$$

$$+ \frac{1}{\varphi_1^2 + \varphi_2^2 + \varphi_3^2} (\varphi_3\varphi_2' - \varphi_2\varphi_3') + O(\delta^2),$$

m_+ : Local mass of heavy fermion

- Contribution of ${\rm arg}[\rho_{tc}]$ is negligibly small (below ~0.4%).

$$|M_{11}|/|M_{22}| \simeq |M_{12}|/|M_{22}| \equiv \delta \lesssim 0.06$$

Inconsistent with Fuyuto, Hou and Senaha, PLB 776 402 (2018)
given by VEV insertion approximation (VIA)

Previous results

- Both results are under CP conserving VEVs $\varphi_1, \varphi_2 \in \mathbb{R}$.

Top-charm mixing

Fuyuto, Hou and Senaha, PLB 776 402 (2018)

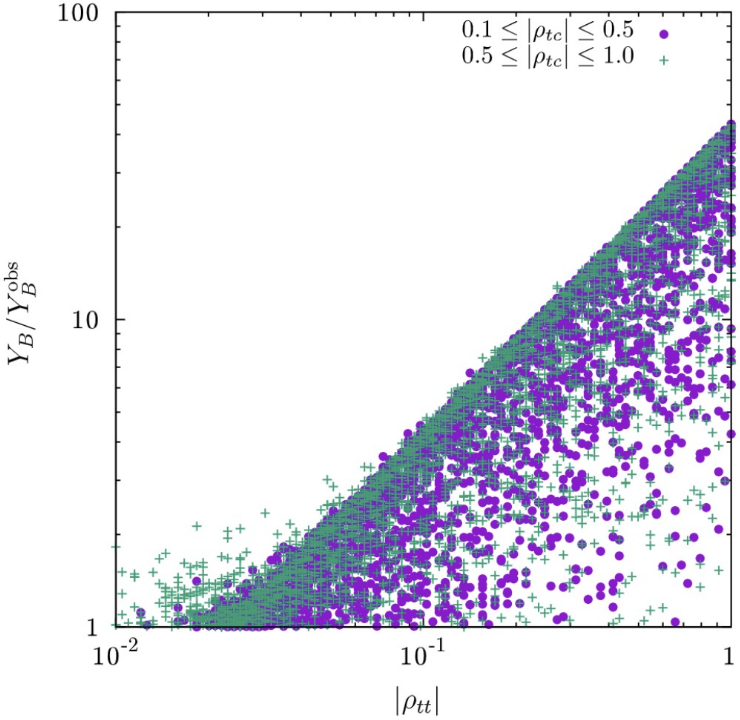

Fig. 2. Impact of ρ_{tt} and ρ_{tc} on Y_B, where the phases ϕ_{tt} and ϕ_{tc} are scanned over 0 to 2π, with other parameters randomly chosen (see text for details). The purple (green) points are for $0.1 \le |\rho_{tc}| \le 0.5$ ($0.5 \le |\rho_{tc}| \le 1.0$).

Tau-mu mixing

Chiang, Fuyuto and Senaha, PLB 762 315 (2016)

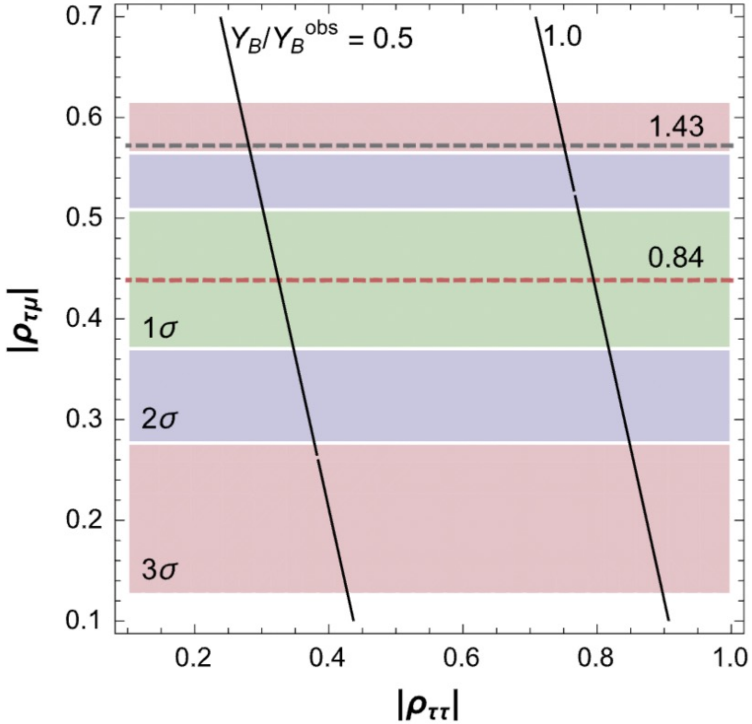

Fig. 2. Contours of $Y_B/Y_B^{\rm obs}$, Br($h \to \mu\tau$) and δa_μ in the ($|\rho_{\tau\tau}|$, $|\rho_{\tau\mu}|$) plane. We set $m_H = 350$ GeV, $m_A = m_{H^\pm} = 400$ GeV, $M = 100$ GeV, $c_{\beta-\alpha} = 0.006$, $|\rho_{\tau\mu}| = |\rho_{\mu\tau}|$, $\phi_{\tau\mu} = -5\pi/4$, $\phi_{\mu\tau} = \pi/4 - \phi_{\tau\mu}$ and $\phi_{\tau\tau} = \pi/2$. (For interpretation of the references to color in this figure, the reader is referred to the web version of this article.)

VIA source terms

- Boltzmann equation for fermion with field theoretical approach A. Riotto (1995), (1997), (1998)

$$\partial_\mu^X j_\psi^\mu = -\int d^3\boldsymbol{w} \int_{-\infty}^{T} dw^0 \, \mathrm{Tr}\Big[\Sigma_\psi^>(X,w)G_\psi^<(w,X) - \Sigma_\psi^<(X,w)G_\psi^>(w,X) - G_\psi^>(X,w)\Sigma_\psi^<(w,X) + G_\psi^<(X,w)\Sigma_\psi^>(w,X)\Big],$$

- CP violations are included in self energy

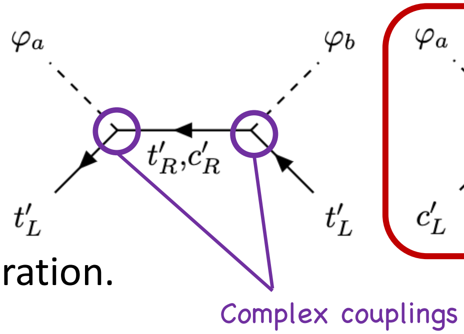

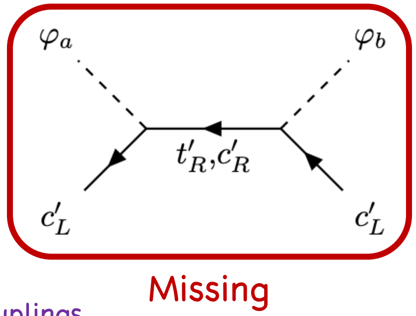

Prime means weak basis

Fuyuto, Hou and Senaha, PLB 776 402 (2018) does not contain contribution of 2nd generation.

- As Fuyuto, Hou and Senaha ,assuming CP conserving VEVs $\varphi_1, \varphi_2 \in \mathbb{R}$

Source of top in weak basis $-\mathcal{L}_y \supset \overline{u'_{i,L}} \left(Y_{1,ij}\phi_1^{0*} + Y_{2,ij}\phi_2^{0*}\right) u'_{j,R},$

$$V_L(Y_1 + Y_2)V_R^\dagger = \sqrt{2}Y_{\mathrm{diag}},$$
$$V_L(-Y_1 + Y_2)V_R^\dagger = \sqrt{2}\rho,$$

$$S_{t'_L} \propto \mathrm{Im}[Y_{1tt}Y_{2tt}^* + Y_{1tc}Y_{2tc}^*] = \mathrm{Im}[(Y_1Y_2^\dagger)_{tt}] = \mathrm{Im}[(V_L^\dagger Y_{\mathrm{diag}}\rho^\dagger V_L)_{tt}]$$

- Consider charm contribution in weak basis

$$S_{t'_L} + S_{c'_L} \propto \mathrm{Im}[(Y_1Y_2^\dagger)_{cc} + (Y_1Y_2^\dagger)_{tt}] = \mathrm{Im}[\mathrm{Tr}(Y_1Y_2^\dagger)] = \mathrm{Im}[\mathrm{Tr}(Y_{\mathrm{diag}}\rho^\dagger)] = -y_c\mathrm{Im}[\rho_{cc}] - y_t\mathrm{Im}[\rho_{tt}],$$

Grossman-Nir bound

Grossman and Nir, PLB 398 163 (1997)

- Mixed Kaon states $|K_{L,S}\rangle = p\,|K^0\rangle \mp q\,|\overline{K^0}\rangle$
- Define amplitudes $A = \langle \pi^0\nu\nu|\, H\, |K^0\rangle\,, \quad \overline{A} = \langle \pi^0\nu\nu|\, H\, |\overline{K^0}\rangle$ and $\lambda = \frac{q}{p}\frac{\overline{A}}{A}$.
- From measurement, $|q/p| \simeq 1$ and $|\lambda| \simeq 1$.

$\pi^0 \sim (\bar{u}u - \bar{d}d)/\sqrt{2},\ \pi^+ \sim \bar{d}u,$
$K^0 \sim \bar{s}d,\ K^+ \sim \bar{s}u$

- Using isospin symmetry relation $A(K^0 \to \pi^0\nu\nu) = \frac{1}{\sqrt{2}} A(K^+ \to \pi^+\nu\nu)$,

  we can find $\frac{\Gamma(K_L \to \pi^0\nu\nu)}{\Gamma(K^+ \to \pi^+\nu\nu)} \simeq \sin^2\theta$, where $\lambda = e^{2i\theta}$.

- We obtain upper bound

  $$\mathrm{Br}(K_L \to \pi^0\nu\nu) \lesssim 4 \times \mathrm{Br}(K^+ \to \pi^+\nu\nu)$$

  with $\tau_{K_L}/\tau_{K^+} \simeq 4.2$.

- SM predictions J. Buras et.al. JHEP 11 (2015) 033

$$\mathrm{Br}(K^+ \to \pi^+\nu\nu)_{\mathrm{SM}} = (8.4 \pm 1.0) \times 10^{-11}$$
$$\mathrm{Br}(K_L \to \pi^0\nu\nu)_{\mathrm{SM}} = (3.4 \pm 0.6) \times 10^{-11}$$

fig. from PDG (2022)

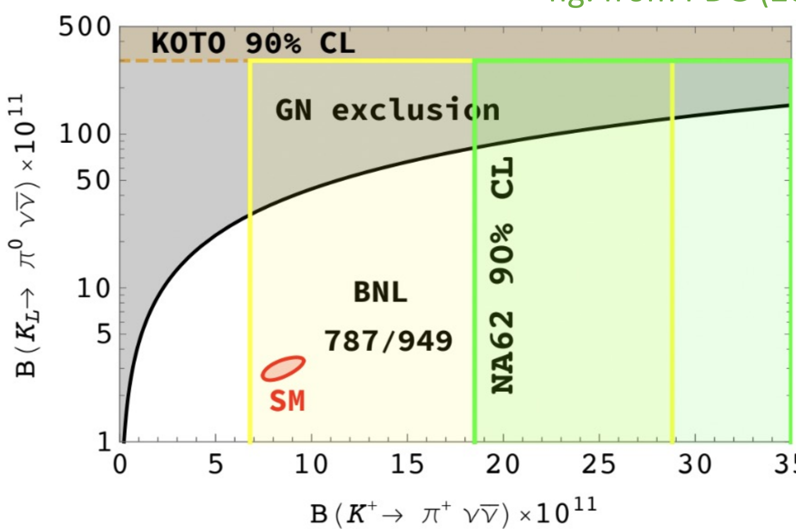

Direct CP violation in Kaon decay

- K_L (K_S) coincides with CP-odd (CP-even) state if CP is conserved.

✗ $K_L \to 2\pi$
○ $K_S \to 2\pi$

- Mixed Kaon states $|K_{L,S}\rangle = p\,|K^0\rangle \mp q\,|\overline{K^0}\rangle$

I : Isospin of two pion system

$$\epsilon' \equiv \frac{\langle I=2|\,T\,|K_L\rangle\,\langle I=0|\,T\,|K_S\rangle - \langle I=2|\,T\,|K_S\rangle\,\langle I=0|\,T\,|K_S\rangle}{\sqrt{2}\,\langle I=0|\,T\,|K_S\rangle^2}$$

$$\propto \langle I=2|\,T\,|K^0\rangle\,\langle I=0|\,T\,|\overline{K^0}\rangle - \langle I=2|\,T\,|\overline{K^0}\rangle\,\langle I=0|\,T\,|K^0\rangle$$

rephasing invariant quantity
represent direct CP violation

$$\frac{\epsilon'}{\epsilon} = -\frac{\omega}{\sqrt{2}|\epsilon_K|}\left[\frac{\mathrm{Im}A_0}{\mathrm{Re}A_0}(1-\Omega_{\mathrm{eff}}) - \frac{1}{a}\frac{\mathrm{Im}A_2}{\mathrm{Re}A_2}\right]$$

a, Ω_{eff} : Isospin breaking effects
$\omega = \langle 2|T|K^0\rangle / \langle 0|T|K^0\rangle$

$$\frac{\epsilon'}{\epsilon} = \left(\frac{\epsilon'}{\epsilon}\right)_{\mathrm{SM}} + \left(\frac{\epsilon'}{\epsilon}\right)_{\mathrm{NP}},$$

$$\left(\frac{\epsilon'}{\epsilon}\right)_{\mathrm{NP}} \simeq \frac{G_F\omega}{2|\epsilon_K|\mathrm{Re}A_0} \times \sum_{i,j}\langle Q_i(\mu)\rangle U_{ij}(\mu,\mu_{\mathrm{NP}})\mathrm{Im}s_i(\mu_{\mathrm{NP}}),$$

Kitahara, Nierste and Tremper (2016)

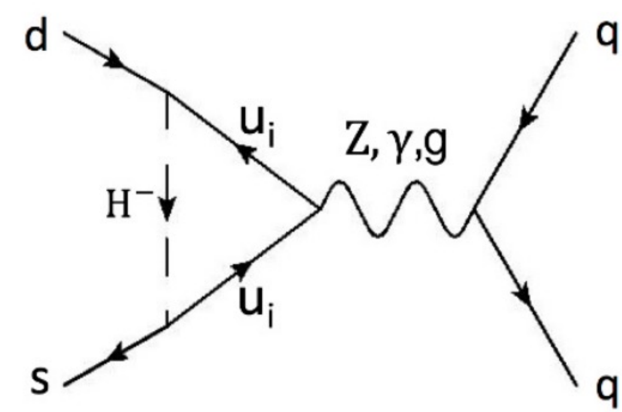

This operator also causes $K \to \pi\nu\nu$ decays.

- Hadronic matrix elements with lattice results

$$\left(\frac{\epsilon'}{\epsilon}\right)_{\mathrm{SM}} = (21.7 \pm 8.4) \times 10^{-4}$$

Blum et. al. (2015), Abbott et. al. (2020)

Collider constraints

- The most stringent constraints to ρ_{tc}

  $cg \to tH_2/H_3 \to tt\bar{c}$

  Same sign multi lepton signal

  CMS, Eur. Phys. J. C 78 140 (2018)
  CMS, Eur. Phys. J. C 80 75 (2020)

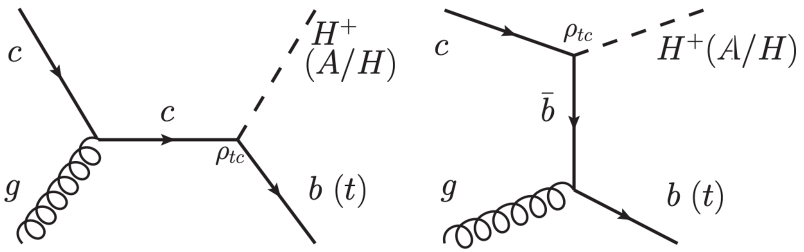

Fig. from Hou, Modak and Plehn (2021)

- Due to interference b/w $cg \to tH_2 \to ttc$ and $cg \to tH_3 \to ttc$, total cross section vanishes with $m_{H_2} = m_{H_3}$ and $\Gamma_{H_2} = \Gamma_{H_3}$. Kohda, Modak, and Hou, Phys. Lett. B 776 379 (2018) Kohda, Modak, and Hou, Phys. Lett. B 786 212 (2018)

- Difference of widths is small as $O(0.1)$ GeV, so that cross section is efficiently small.

  Solid : H_2
  Dashed : H_3

- Other collider constraints relevant to ρ_{tt} are weakened by large ρ_{tc}.

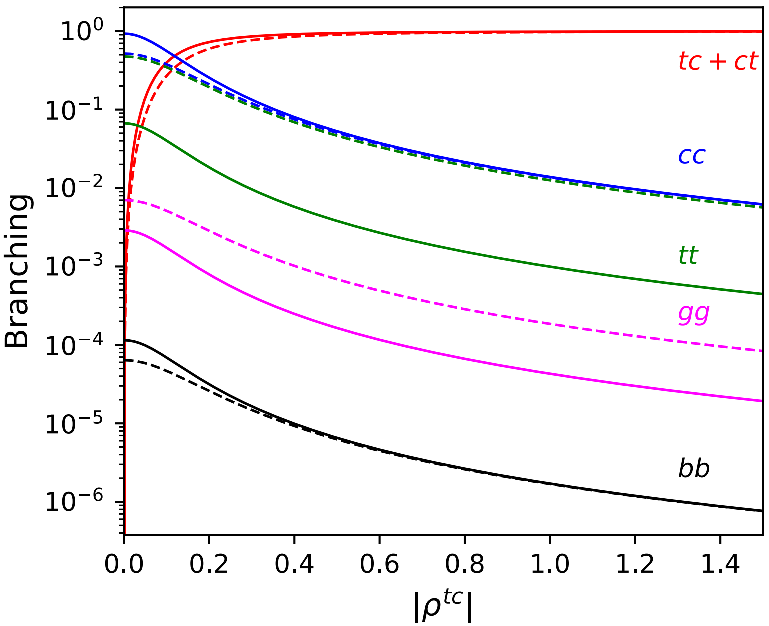

About BAU (top transport)

CP violating bubble

Order parameter $h_1 = h, h_2 = H\cos\varphi_H, h_3 = H\sin\varphi_H$

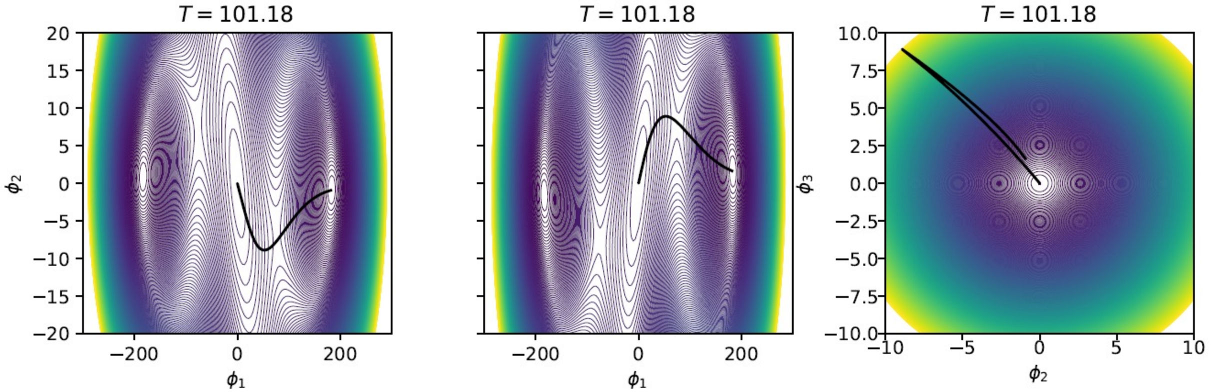

Black line is the path of PT.

Vertical: Heavy scalar mode
Horizontal: Light scalar mode

Large VEVs $\phi_{2,3}$ during PT are needed for BAU.

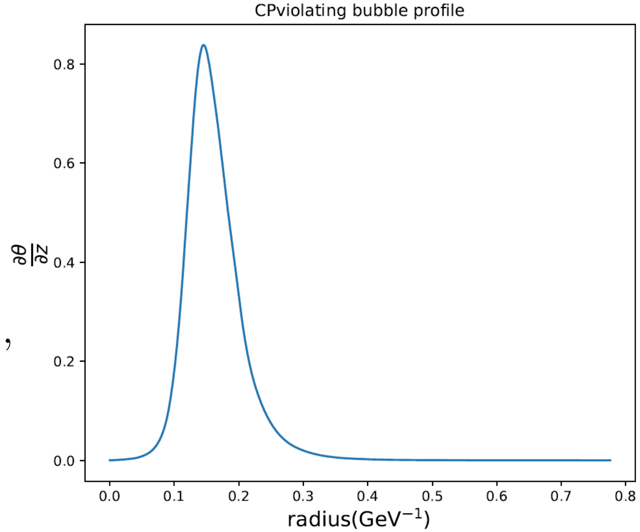

Localized top phase

$$\partial_z\theta(z) = -\frac{\varphi_H^2}{\varphi_{H_1}^2 + \varphi_H^2}\partial_z\theta_H - \partial_z \arctan\left(\frac{|\zeta_u|\varphi_H \sin(\theta_H + \theta_u)}{\varphi_{H_1} + |\zeta_u|\varphi_H \cos(\theta_H + \theta_u)}\right),$$

$$\varphi_H \equiv \sqrt{\varphi_{H_2}^2 + \varphi_{H_3}^2}, \quad \theta_H = \arctan(\varphi_{H_2}/\varphi_{H_3}),$$

We used `CosmoTransitions` to calculate the bubble wall profile.

Wainwright, Comput. Phys. Commun. 183 (2011)

Estimation of baryon density

<u>Top transport scenario</u> Fromme and Huber, JHEP 03 (2007)

CP violating source is the top quark which has large yukawa coupling.

Localized top quark mass $$m_t(z) = \frac{y_t}{\sqrt{2}} v(z) e^{i\theta(z)}$$

Higgs potential at finite temperature determines the bubble profile.

$v(z), \theta(z), T_n, L_w, \ldots$

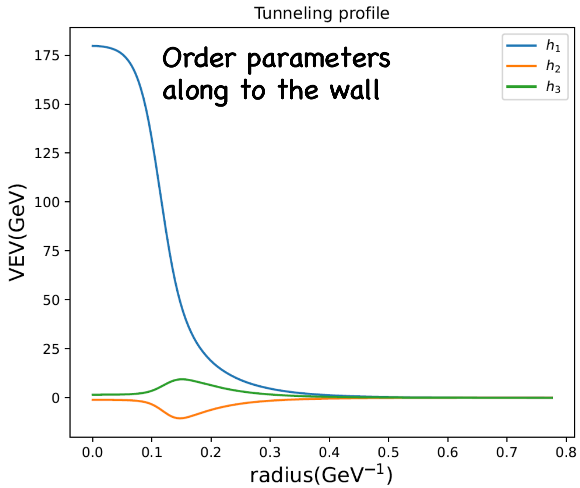

"Semi classical force mechanism" (WKB method) Cline, Joyce and Kainulainen, JHEP 07 (2000); Cline and Kainulainen Phys. Rev. D 101 (2020)

Boltzmann equation $$(\partial_t + \boldsymbol{v}_g \cdot \partial_{\boldsymbol{x}} + \boldsymbol{F} \cdot \partial_{\boldsymbol{p}}) f_i = C[f_i, f_j, \ldots]$$

Overall signs are flipped between particles and anti-particles.

$$v_g = \frac{p_z}{E_0}\left(1 \pm s\frac{\theta'}{2}\frac{m^2}{E_0^2 E_{0z}}\right)$$

$$F_z = -\frac{(m^2)'}{2E_0} \pm s\frac{(m^2\theta')'}{2E_0 E_{0z}} \mp s\frac{\theta' m^2 (m^2)'}{4E_0^3 E_{0z}}$$

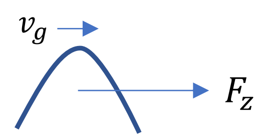

Particle distributions are small away from its equilibrium form

$$f_i = \frac{1}{e^{\beta[\gamma_w(E_i + v_w p_z) - \mu_i]} \pm 1} + \delta f_i$$

Transport equations

Boltzmann equation $(\partial_t + \boldsymbol{v}_g \cdot \partial_{\boldsymbol{x}} + \boldsymbol{F} \cdot \partial_{\boldsymbol{p}}) f_i = C[f_i, f_j, \ldots]$

Overall signs are flipped between particle and anti-particle.

$$v_g = \frac{p_z}{E_0}\left(1 \pm s\frac{\theta'}{2}\frac{m^2}{E_0^2 E_{0z}}\right)$$

$$F_z = -\frac{(m^2)'}{2E_0} \pm s\frac{(m^2\theta')'}{2E_0 E_{0z}} \mp s\frac{\theta' m^2 (m^2)'}{4E_0^3 E_{0z}}$$

Particle distributions are small away from its equilibrium form $f_i = \dfrac{1}{e^{\beta[\gamma_w(E_i + v_w p_z) - \mu_i]} \pm 1} + \delta f_i$

Boltzmann equation can be expanded by small wall velocity, and after integrated in momentum,

$$v_w K_1 \mu' + v_w K_2 (m^2)' \mu + u' - \langle \boldsymbol{C}[f] \rangle = 0$$

(K series are z-dependent functions)

$$-K_4 \mu' + v_w \tilde{K}_5 u' + v_w \tilde{K}_6 (m^2)' u - \left\langle \frac{p_z}{E_0} \boldsymbol{C}[f] \right\rangle = S_\theta \qquad S_\theta = -v_w K_8 (m^2\theta')' + v_w K_9 \theta' m^2 (m^2)'$$

Plasma flame

$$\frac{\partial n_B}{\partial t} = \frac{3}{2}\Gamma_{\rm sph}\left(3\mu_{B_L} - \frac{A}{T^3} n_B\right)$$

Integrated in wall flame

$$\eta_B = \frac{405\Gamma_{\rm sph}}{4\pi^2 v_w g_* T} \int_0^\infty dz\, \mu_{B_L} f_{\rm sph} e^{-45\Gamma_{\rm sph} z/(4v_w)}$$

$$f_{\rm sph}(z) = \min\left(1, \frac{2.4T}{\Gamma_{\rm sph}} e^{-40v(z)/T}\right)$$

Velocity dep. of baryon density

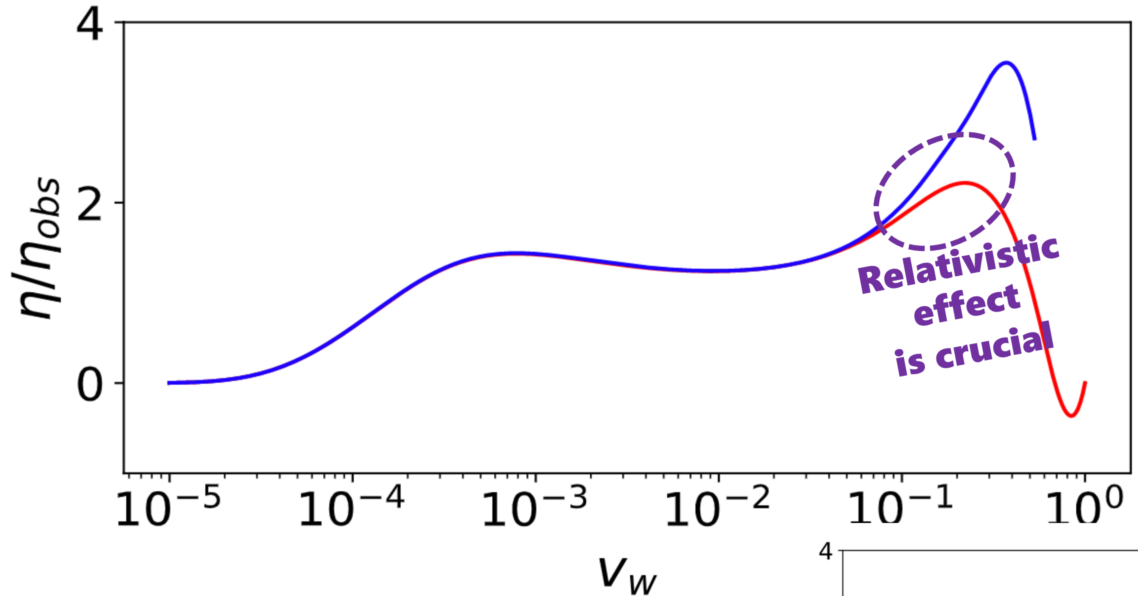

For the predictable GWs, relativistic effects must be included.

Blue: Fromme and Huber, JHEP 03 (2007)

Red: Cline and Kainulainen, Phys. Rev. D 101 (2020)

Velocity dependences differ in nucleation temperatures.

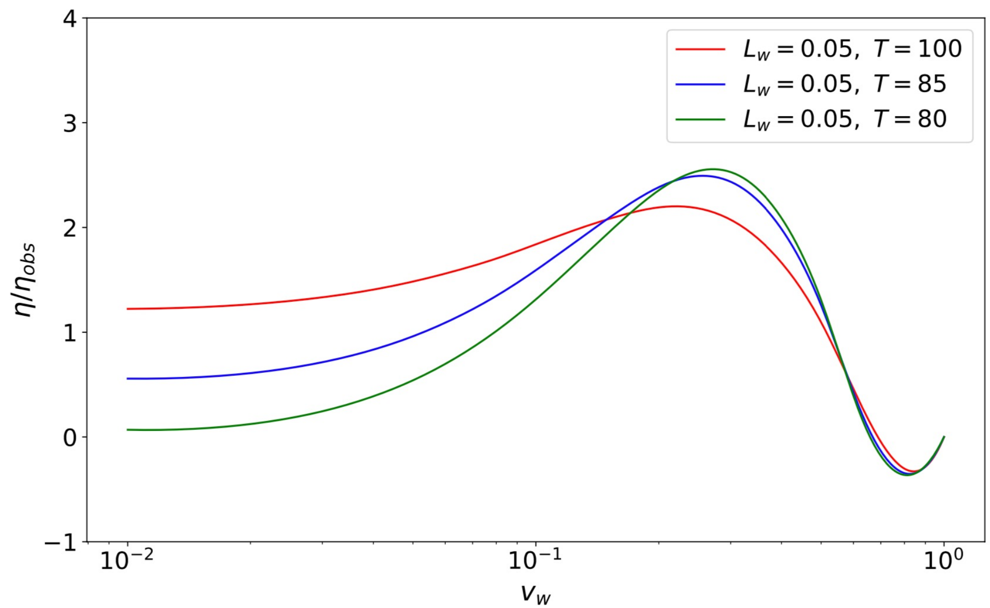

Wall width dependence of BAU

Cline and Laurent, Phys. Rev. D 104 (2021)

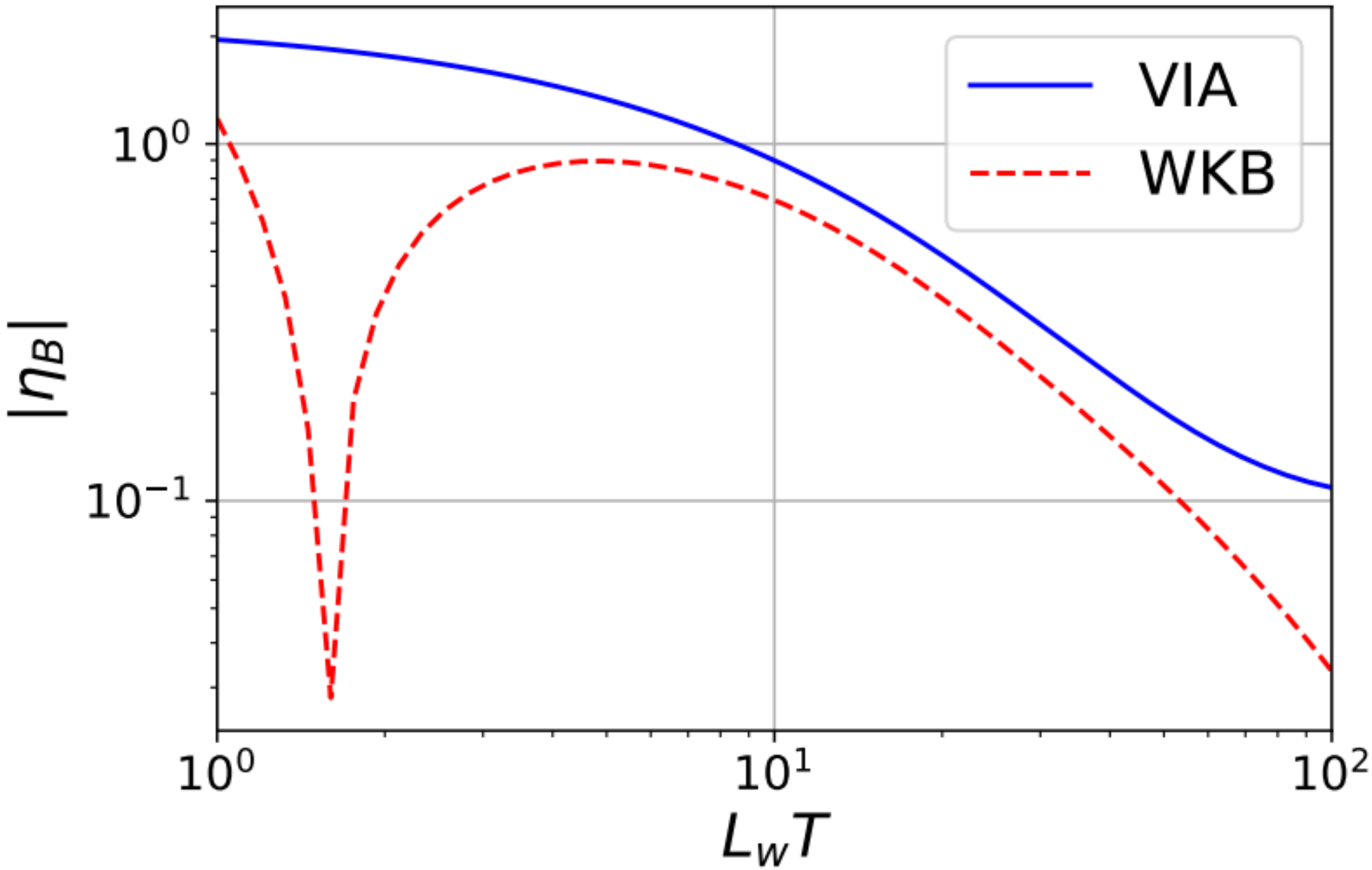

WKB formalism has accidental zero-crossing behavior.

Supplement figures

Velocity dependence of BAU

Baryon asymmetry in the relativistic bubble wall velocity Cline and Kainulainen, Phys. Rev. D 101 (2020)

Assuming the velocity as a free parameter

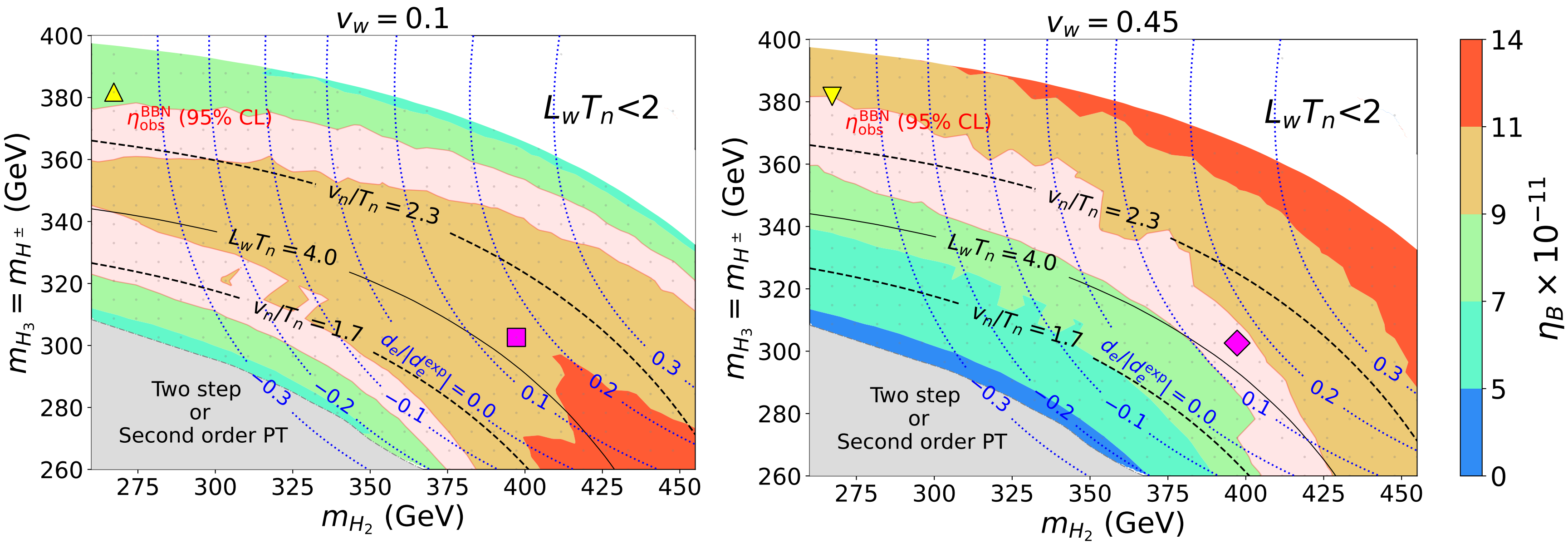

Strongly first order PT (except for gray region)

$$M = 30\,\mathrm{GeV},\ \lambda_2 = 0.1,\ |\lambda_7| = 0.8,\ \theta_7 = -0.9,$$
$$|\zeta_u| = |\zeta_d| = |\zeta_e| = 0.18,\ \theta_u = -2.7,\ \delta_d = 0,\ \delta_e = -0.04.$$

The observed BAU (pink) $\eta_{obs}^{\rm BBN} \equiv \dfrac{n_B}{s} = 8.2\text{–}9.2 \times 10^{-11}$

Electron EDM (blue dotted) $|d_e^{\rm exp}| < 1.1\times10^{-29} e$ cm

Andreev *et al.* [ACME] Nature 562 (2018)

green: relate to the BAU
blue: relate to the eEDM
purple: relate to the both

We set four benchmarks :

- △ BP1a: small velo. + strongly PT
- ▽ BP1b: large velo. + strongly PT
- ■ BP2a: small velo. + weakly PT
- ◆ BP2b: large velo. + weakly PT

Effective potential

Thermal resummation → Parwani scheme
1 loop potential → Landau gauge ($\xi = 0$)

Renormalization condition
→ MS-bar scheme ($\lambda_{2,7}, M$) + On-shell scheme (other parameters)

$$\left.\frac{\partial V}{\partial h_i}\right|_{\substack{h_1=v\\h_2=h_3=0}} = 0$$

$$\left.\frac{\partial^2 V}{\partial h_i \partial h_j}\right|_{\substack{h_1=v\\h_2=h_3=0}} = \mathcal{M}_{ij}^2$$

We used cutoff $m_{NG} = m_{IR} \sim 1$ GeV to avoid IR divergence.

K. Enomoto, S. Kanemura, and Y.M, JHEP 01 (2022) 104

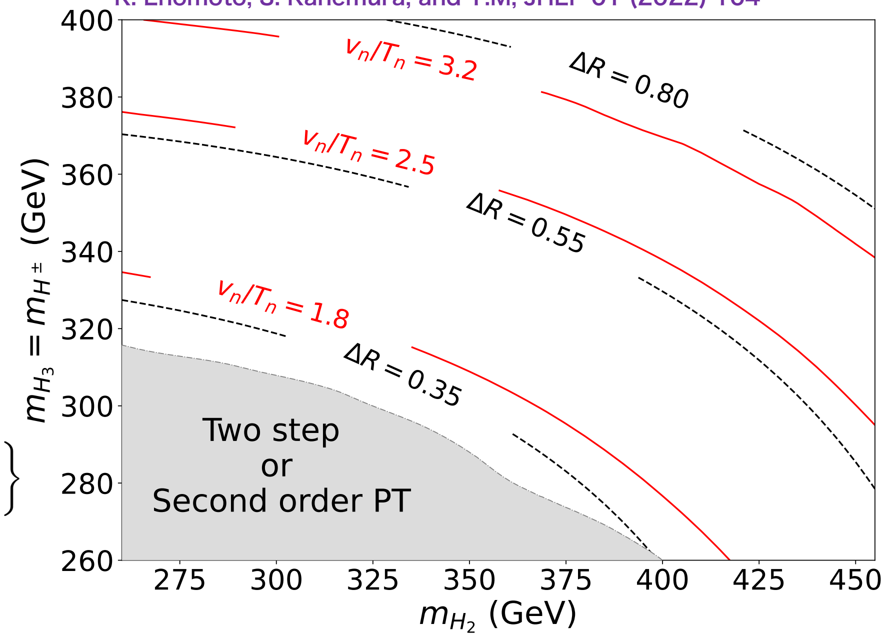

Higgs triple coupling at 1 loop level

$$\Delta R \equiv \frac{\lambda_{hhh} - \lambda_{hhh}^{\rm SM}}{\lambda_{hhh}^{\rm SM}}$$
$$\simeq \frac{1}{12\pi^2 v^2 m_{H_1}^2}\left\{2\frac{(m_\pm^2 - M^2)^3}{m_\pm^2} + \frac{(m_{H_2}^2 - M^2)^3}{m_{H_2}^2} + \frac{(m_{H_3}^2 - M^2)^3}{m_{H_3}^2}\right\}$$

Relation between ϕ/T and ΔR (right figure)

EW Phase transition

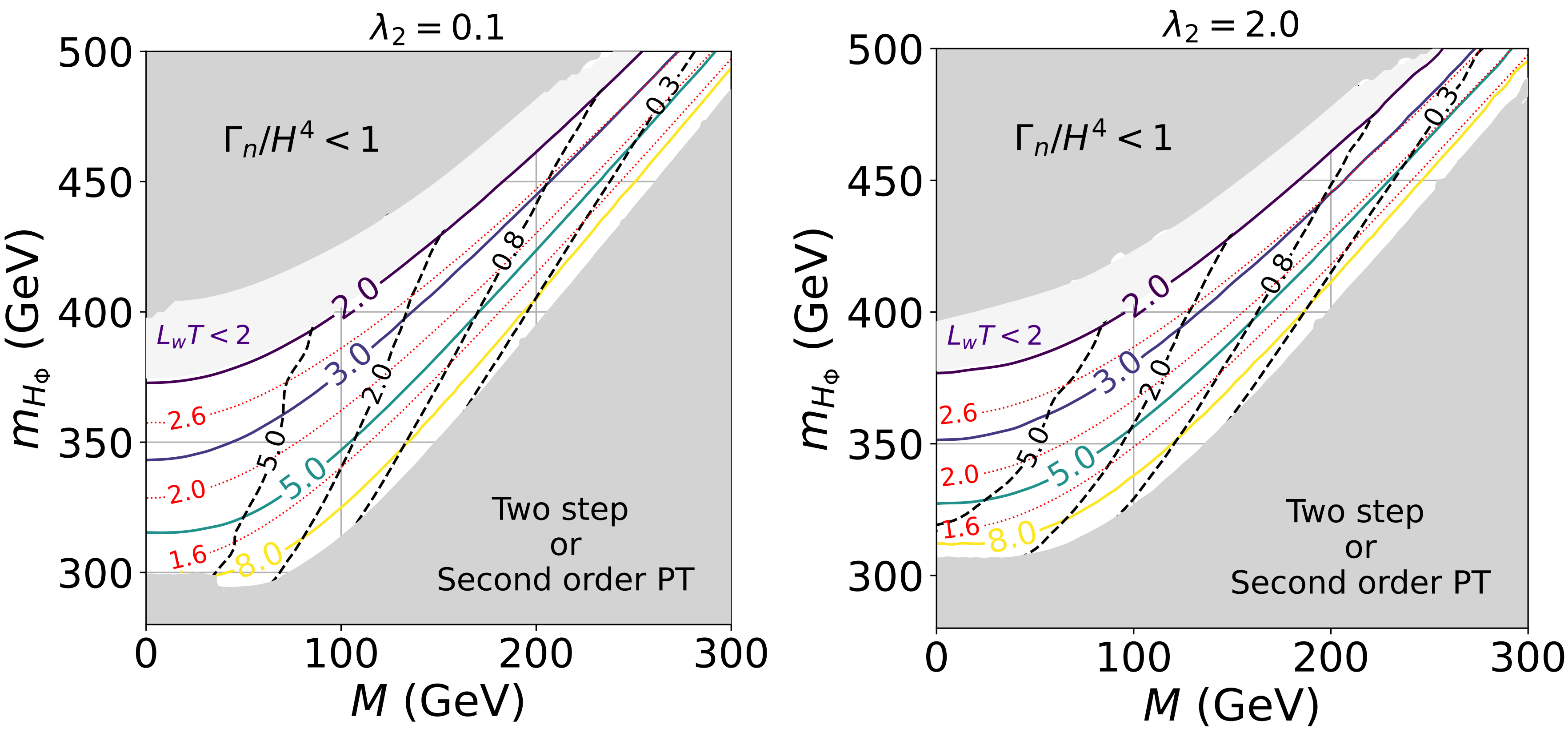

When M and λ_2 are large, $\partial_z\theta|_{max}$ becomes small.

Red dotted : v_n/T_n
Color solid : L_wT
Black dashed : $\partial_z\theta|_{max}$

Source term $\quad S_\theta = -v_w K_8(m^2\theta')' + v_w K_9 \theta' m^2 (m^2)'$

Velocity dep. of efficiency factor

Efficiency $\kappa_v(\alpha, v_w)$ means how much the latent heat is converted to the sound waves.

No hydrodynamical eq. exists when $\alpha \sim 1,\ v_w \lesssim c_s$. Espinosa *et al.* JCAP 06 (2010)

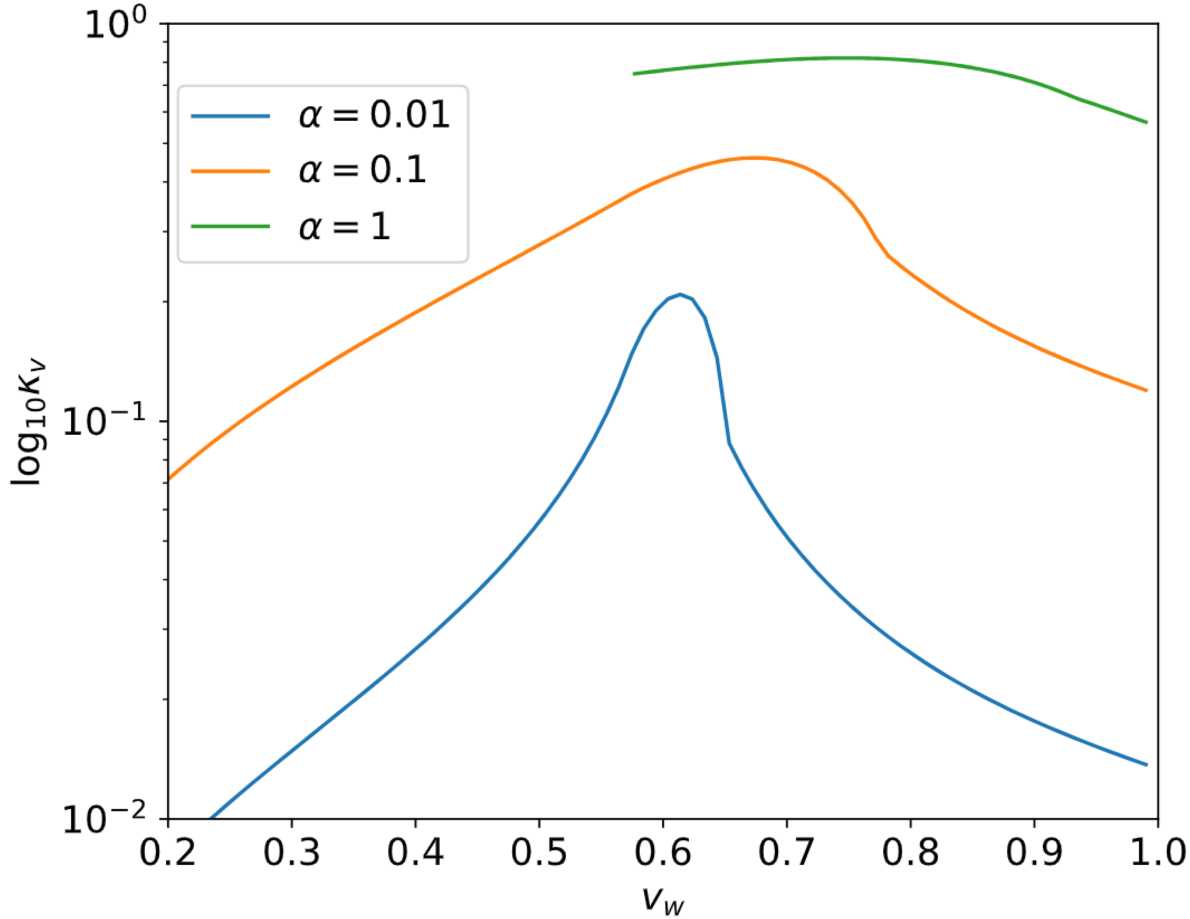

Gravitational waves from EWPT

			v_w	m_{H_2}	$m_{H_3,H^\pm}$	M	v_n/T_n	$L_w T_n$	η_B	ΔR	$\sigma\mathcal{B}(H_1 \to \gamma\gamma)$
Strongly PT	small velo. △	BP1a	0.1	267 GeV	381 GeV	30 GeV	2.4	2.6	7.8×10^{-11}	0.61	104 ± 5 fb
	large velo. ▽	BP1b	0.45						9.1×10^{-11}		
Weakly PT	small velo. ■	BP2a	0.1	397 GeV	302 GeV	30 GeV	2.0	4.1	10.8×10^{-11}	0.44	
	large velo. ◆	BP2b	0.45						9.0×10^{-11}		

Gravitational wave spectra

Grojean and Servant, Phys. Rev. D 75 (2007);
Kakizaki, Kanemura and Matsui, Phys. Rev. D 92 (2015); and more

Sensitivity curves Hashino *et al.* Phys. Rev. D 99 (2019)

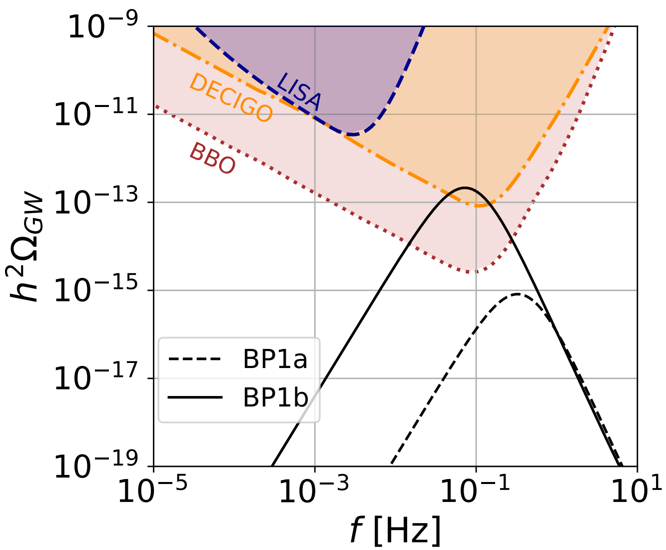

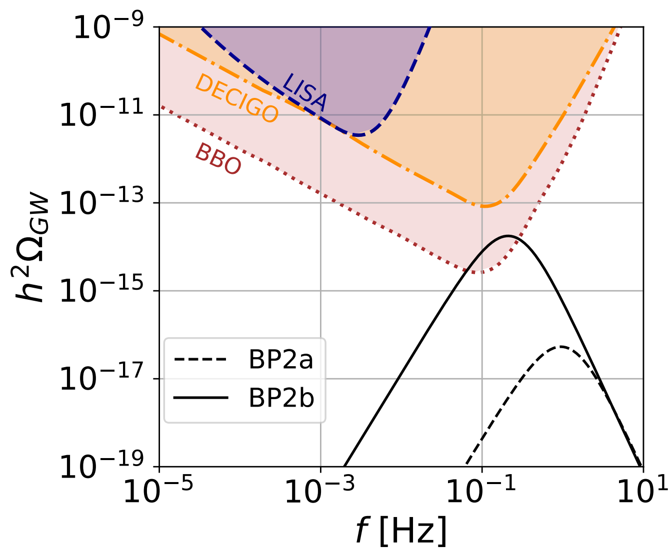

Strong PT and large velocity are needed.

BP1b and BP2b can also be tested by GW observation.

Scatter plot for eEDM and BAU

$$\lambda_2 = 0.1,\ m_\Phi = 350\ \mathrm{GeV},\ M = 30\ \mathrm{GeV},\ v_w = 0.1,$$
$$\theta_u = \theta_d = [0, 2\pi),\ |\zeta_d| = |\zeta_e| = [0, 10],\ |\lambda_7| = [0.5, 1.0],\ \theta_7 = [0, 2\pi).$$

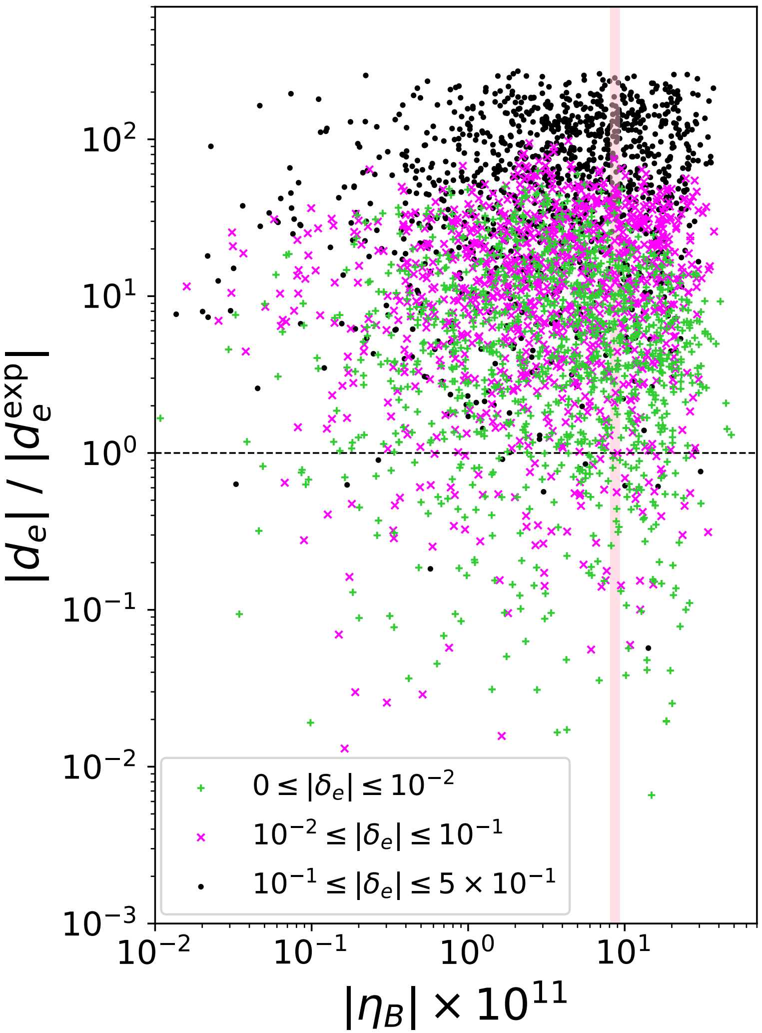

These points are allowed from various constraints.

Fermion loop contributions are proportional to $|\zeta_u||\zeta_e|\sin\delta_e$.
$(\delta_e \equiv \theta_u - \theta_e)$

Many points are satisfied from eEDM data and they generate sufficient BAU.

di-Higgs production at linear collider

Higgs production at e+ e- collider   Abramowicz et al., Eur. Phys. J. C (2017) 77 475

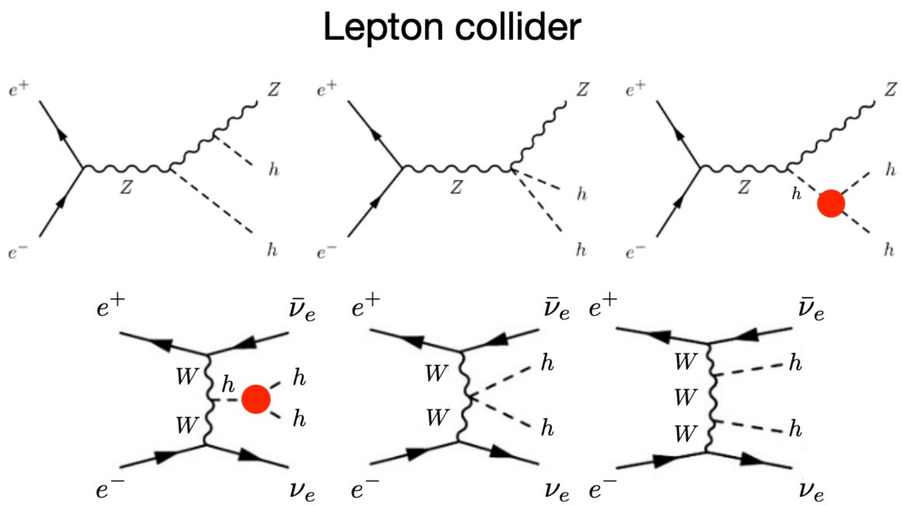

no polarization

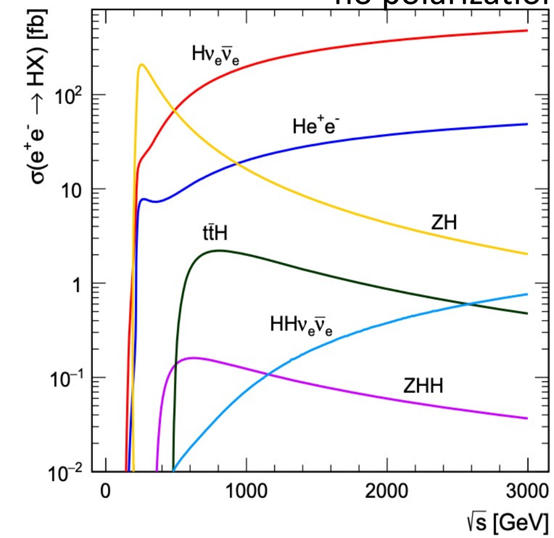

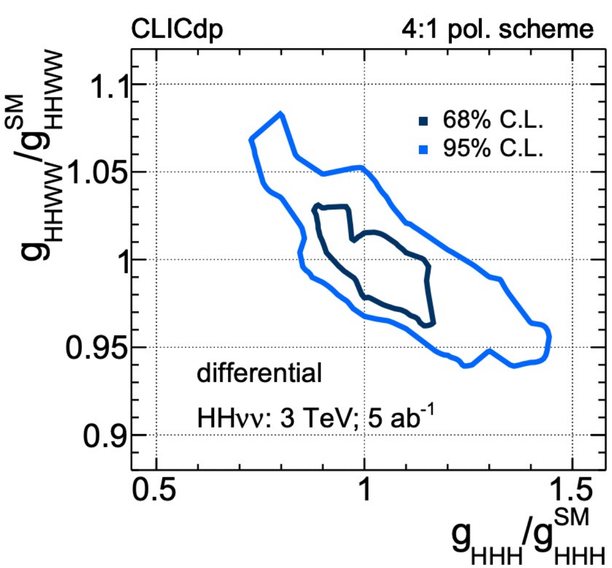

Higgs self coupling at CLIC Stage-3 (3 TeV)

Philipp Roloff *et al.,* Eur. Phys. J. C 80 (2020) 11, 1010

λ_{hhh} measurement at future colliders

de Blas *et al.* JHEP 01(2020)

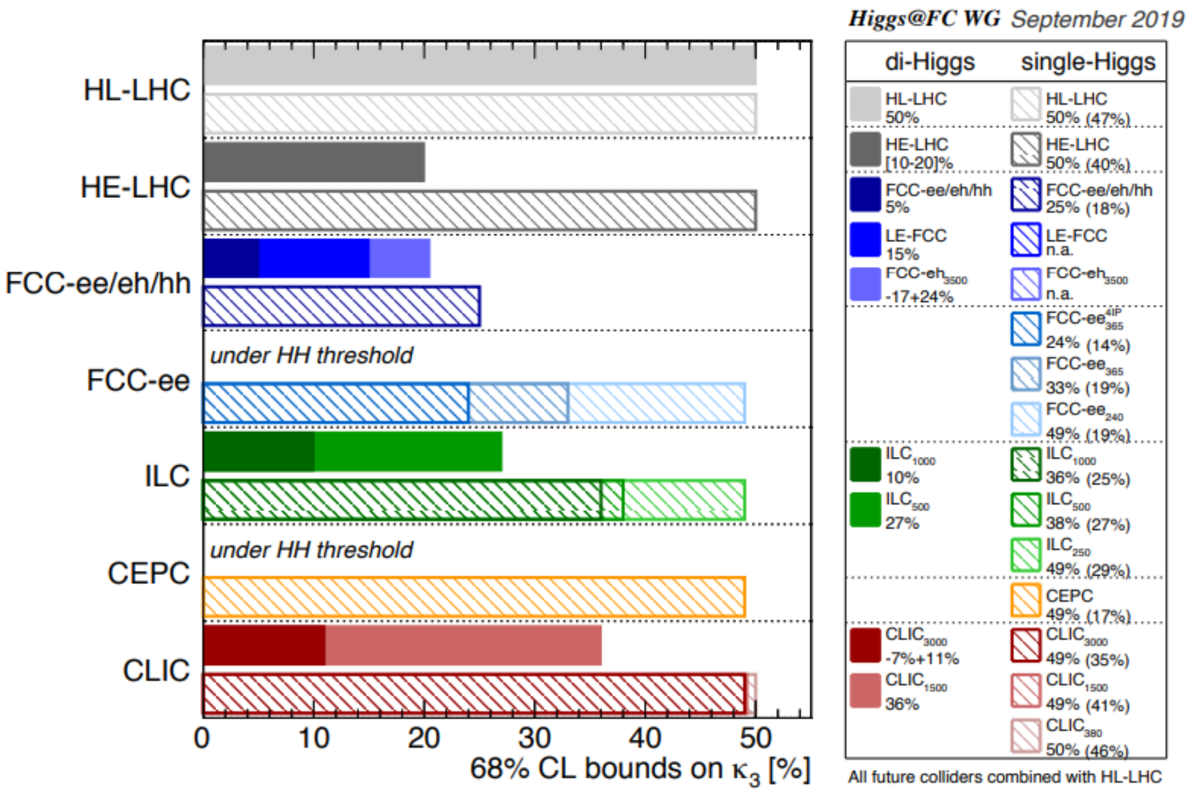

Hadron collider

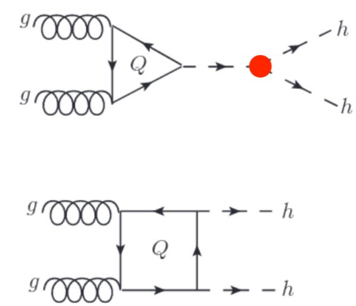

Lepton collider

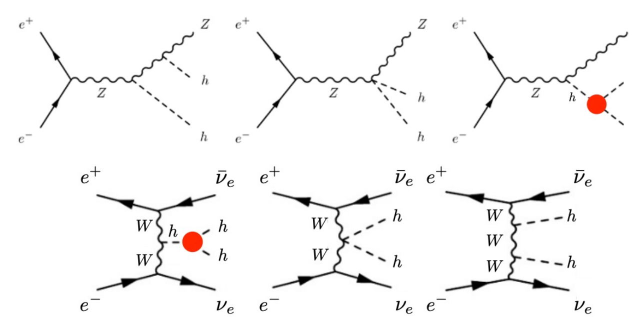

Testing CP violation

- **Future flavor and EDM experiments for testing CPV**

Blue : $B \to X_s\gamma$

Black :

$$\Delta A_{CP} = A_{CP}(B^+ \to X_s^+\gamma) - A_{CP}(B^0 \to X_s^0\gamma)$$

$$A_{CP}(X) \equiv \frac{\Gamma(\bar{X}) - \Gamma(X)}{\Gamma(\bar{X}) + \Gamma(X)}$$

Benzke *et al.* Phys. Rev. Lett. 106 (2011);
Watanuki *et al.* [Belle] Phys. Rev. D 99 (2019);

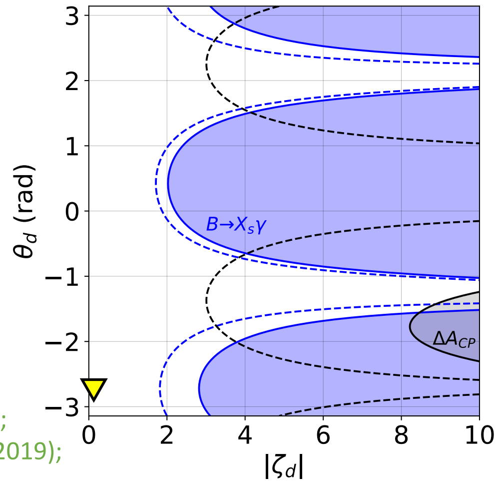

$|d_n| < 1.8{\times}10^{-26} e$ cm

Abel *et al.* [nEDM] (2020)

Red : $d_n + C_W$ case

Gray : $d_n - C_W$ case

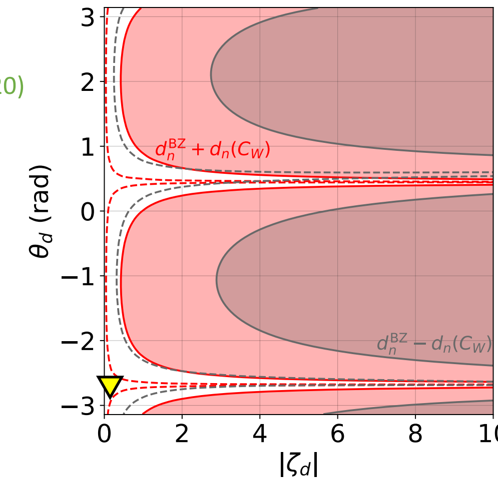

- **CPV in the decays of the neutral scalar bosons** ($|\zeta_d| \ll |\zeta_e|$ case)

Phase of ζ_e would be measured at upgraded ILC

Kanemura, Kubota and Yagyu, JHEP 04 (2021) 144

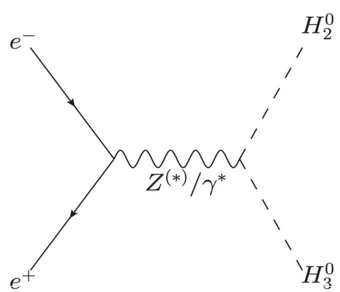

$$H_{2,3} \to \tau^+\tau^- \to X^+\bar{\nu}X^-\nu$$

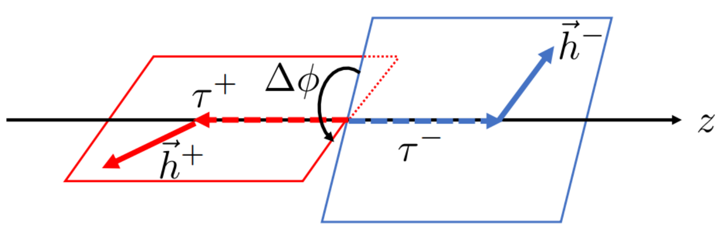

Jeans and Wilson, Phys. Rev. D 98 (2018) 013007

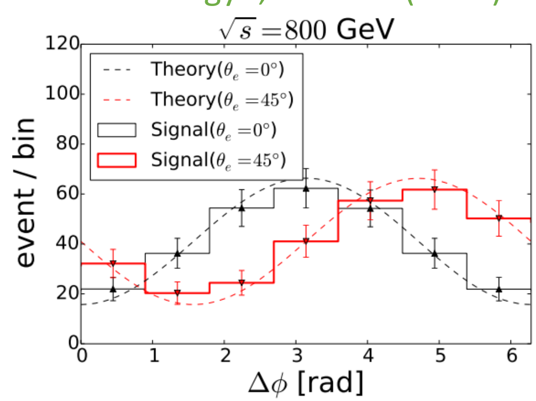

- **Top-charm mixing effects on the BAU** Kanemura and Y.M., arXiv:2303.11252

Constraints on the model

- **Constraints from direct searches and various flavor observables**

Direct search experiments

$H_{2,3} \to \tau\tau$ Aad *et al.* [ATLAS] Phys. Rev. Lett. 125 (2020)

$H_{2,3}(bb) \to \tau\tau$

$H_{2,3} \to tt$ Aaboud *et al.* [ATLAS] Eur. Phys. J. C 78 (2018); Sirunyan *et al.* [CMS] JHEP 04 (2020)

$H^{\pm} \to tb$ Aad *et al.* [ATLAS] JHEP 06 (2021)

$H^{\pm} \to \tau\nu$ Sirunyan *et al.* [CMS] JHEP 07 (2019)

Flavor experiments

$B_d \to \mu\mu$, $B_s \to \mu\mu$, $B \to X_s\gamma$: Amhis *et al.* [HFLAV] Eur. Phys. J. C 81 (2021); Haller *et al.* Eur. Phys. J. C 78 (2018); Aaboud *et al.* [ATLAS] JHEP 04 (2019); Sirunyan *et al.* [CMS] JHEP 04 (2020); Aaij. *et al.* [LHCb] Phys. Rev. D 105 (2022)

$|\zeta_u| = |\zeta_d| = |\zeta_e|$ (Type I 2HDM)

Experimental upper bound $|\zeta_u| \lesssim 0.6$

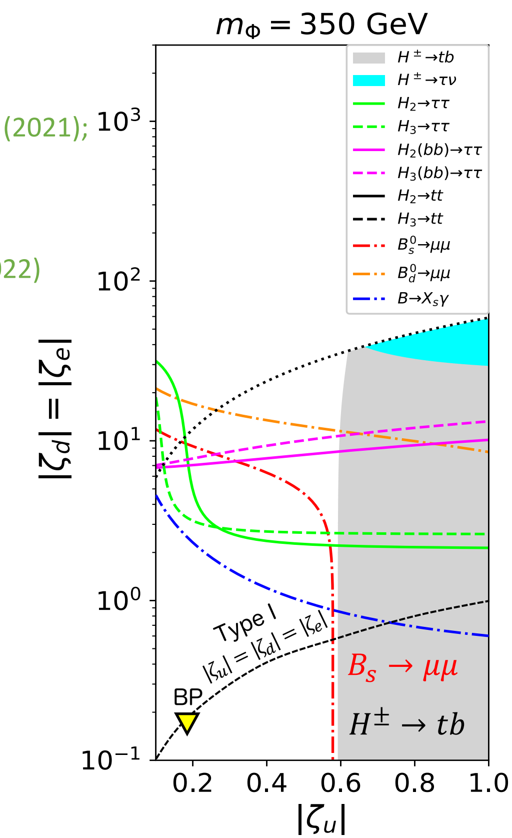

$m_\Phi \equiv m_{H_2} = m_{H_3} = m_{H^\pm}$

- **Important Yukawa interaction for baryogenesis**

$$\mathcal{L}_y \supset \zeta_u^* \frac{\sqrt{2}M_t}{v} \overline{Q_{3L}} \tilde{\Phi}_2 b_R + \text{h.c.},$$

Top transport scenario

Fromme and Huber, JHEP 03 (2007) 049

- **CPV interaction of top quarks to the bubble wall**

Local mass term along to the bubble wall $m_t(z) = \frac{y_t}{\sqrt{2}} v(z) e^{i\theta(z)}$ generates BAU

Higgs to di-photon decay

Non decoupling effect in $H_1 \to \gamma\gamma$

The constraints on the coupling $H_1 H^{\pm} H^{\pm}$

$$m_{H^\pm}^2 = M^2 + \frac{1}{2}\lambda_3 v^2$$

Red line is prediction in the case of $M = 30$ GeV.

SM expected (blue): $\sigma Br(H_1 \to \gamma\gamma) = 116 \pm 5$ fb

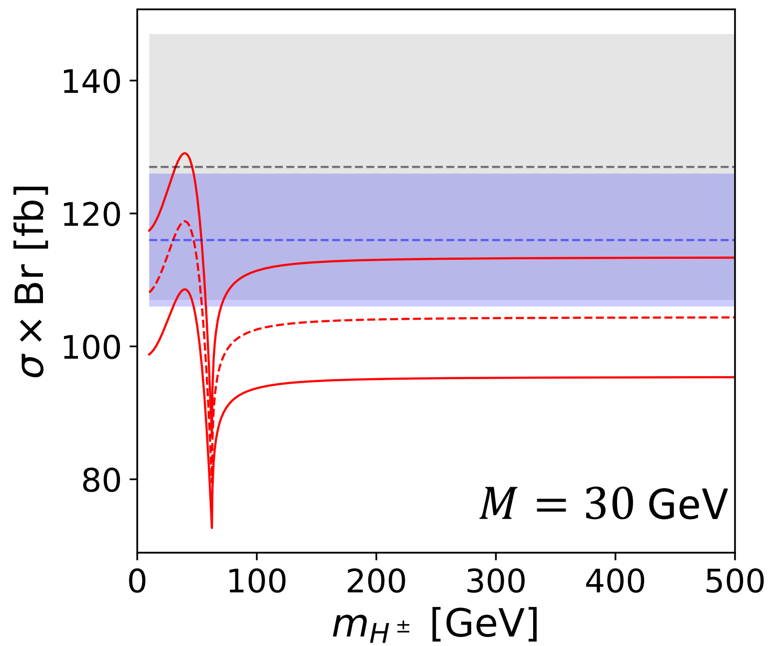

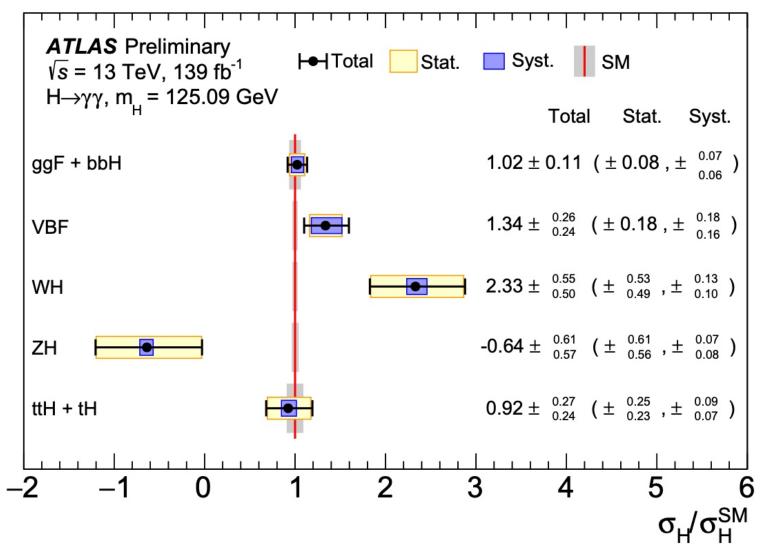

Observed (gray): $\sigma Br(H_1 \to \gamma\gamma) = 127 \pm 10$ fb

σ is inclusive production cross section of H_1.

ATLAS-CONF-2020-026

Neutron EDM

Experimental bound: $|d_n| < 1.8\times10^{-26} e$ cm Abel *et al.* [nEDM] Phys. Rev. Lett. 124 (2020)

ζ_d is restricted from neutron EDM.
The leading graph is chromo Barr-Zee type of down quark.

$d_n \supset$ 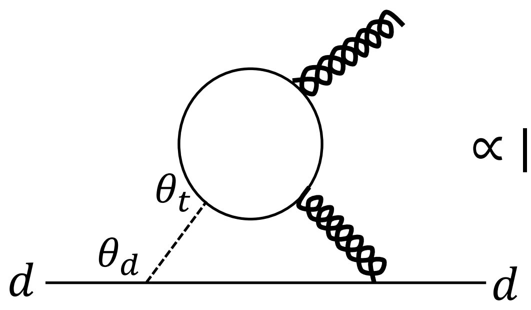 $\propto |\zeta_u||\zeta_d|\sin(\theta_u - \theta_d)$

In BP1

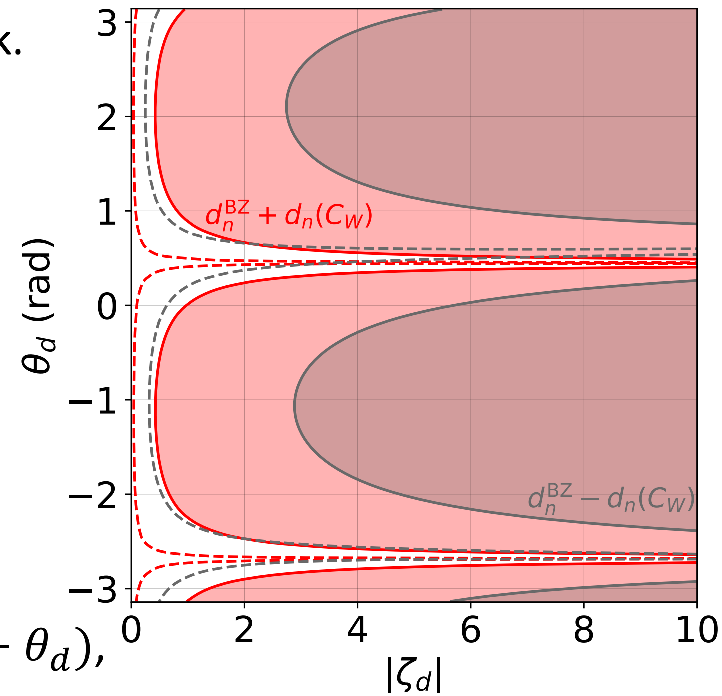

Also, from Weinberg operator $d_n(C_W) \propto |\zeta_u||\zeta_d|\sin(\theta_u - \theta_d)$, but the sign of $d_n(C_W)$ is not determined.

Solid: current
Dashed: expected

Red: $d_n^{BZ} + d_n(C_W)$ case
Gray: $d_n^{BZ} - d_n(C_W)$ case

Destructive interference

Dimension 5 effective operator

$$H_{\rm EDM} = -d_f \frac{\boldsymbol{S}}{|\boldsymbol{S}|}\cdot \boldsymbol{E} \qquad \mathcal{L}_{\rm EDM} = -\frac{d_f}{2}\bar{f}\sigma^{\mu\nu}(i\gamma_5)fF_{\mu\nu}$$

Time reversal

$$\mathcal{T}(\boldsymbol{E}) = \boldsymbol{E}, \mathcal{T}(\boldsymbol{S}) = -\boldsymbol{S}$$

T violation → From CPT theorem, CP is violated.

Two diagrams contribute to the electron EDM in our model.

Experimental bound $|d_e| < 1.1\times 10^{-29} e$ cm

Andreev *et al.* [ACME] Nature 562 (2018)

$d_e \simeq$

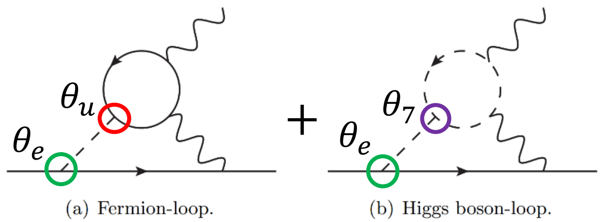

Destructive interference between two independent CP phase

Kanemura, Kubota and Yagyu, JHEP 08 (2020)

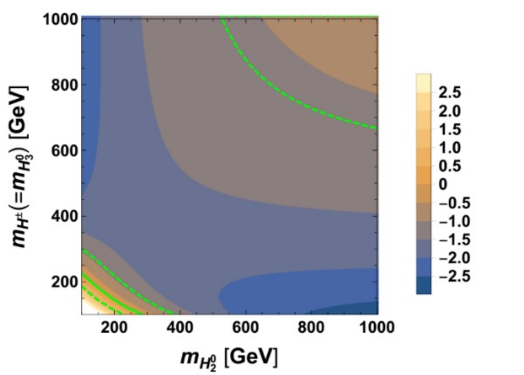

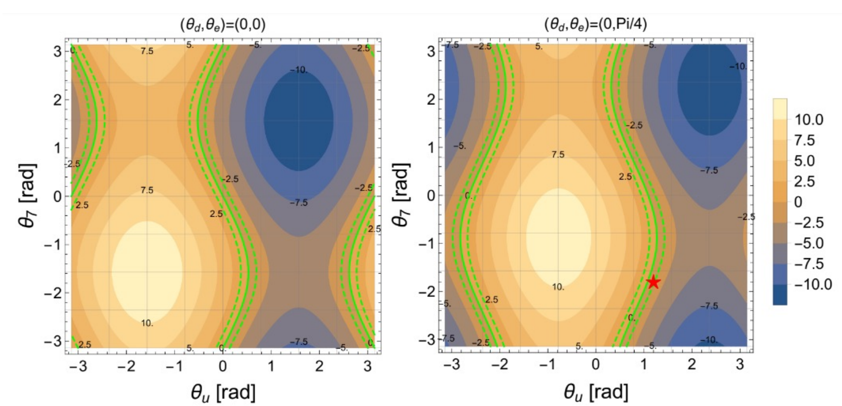

θ_7 and θ_u are important to generate BAU.

Flavor constrarints

Model	ς_d	ς_u	ς_l
Type I	$\cot\beta$	$\cot\beta$	$\cot\beta$
Type II	$-\tan\beta$	$\cot\beta$	$-\tan\beta$
Type X	$\cot\beta$	$\cot\beta$	$-\tan\beta$
Type Y	$-\tan\beta$	$\cot\beta$	$\cot\beta$
Inert	0	0	0

Haller *et al.* Eur. Phys. J. C 78 (2018);

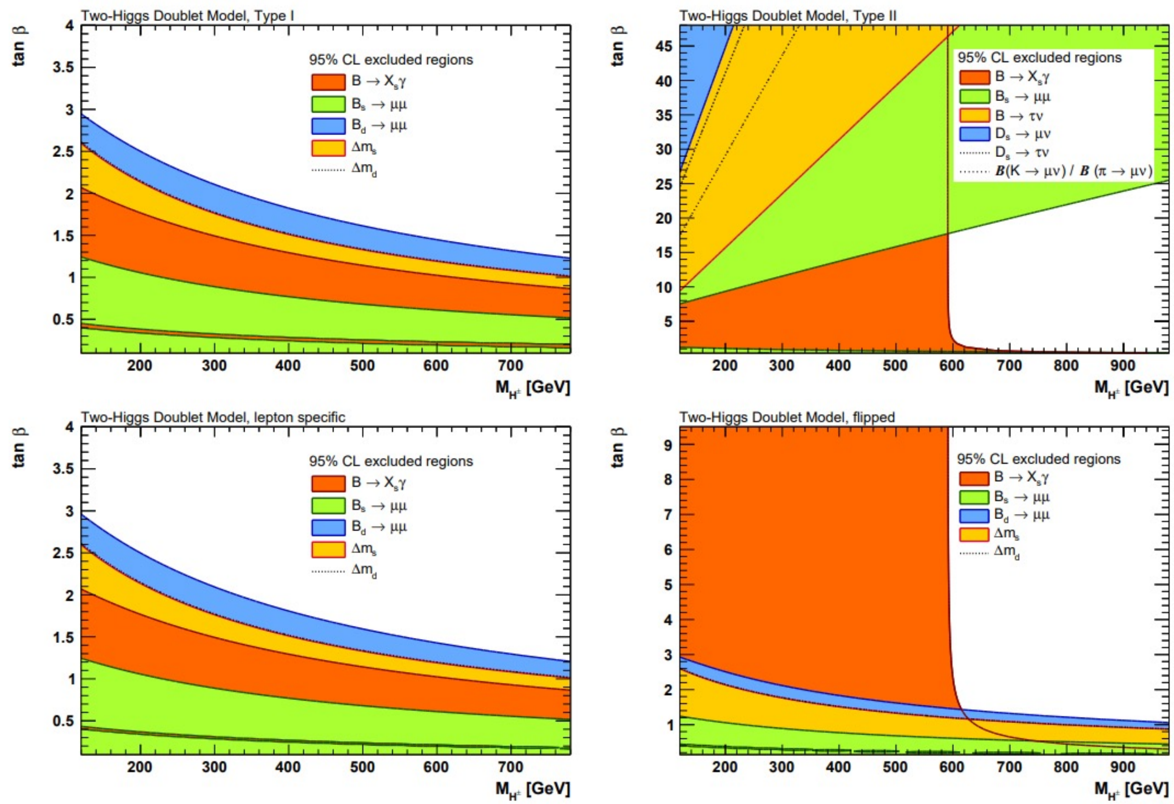

Type Ⅰ like

$$|\zeta_u| = |\zeta_d| = |\zeta_e| = \cot\beta$$

Type X like

$$|\zeta_u| = |\zeta_d| = \cot\beta$$

$$|\zeta_e| = -\tan\beta$$

$$m_{H^\pm} \simeq 300\text{GeV}, |\zeta_u| \lesssim 0.4$$

Collider constraints

Aiko, Kanemura, Kikuchi, Mawatari, Sakurai and Yagyu, Nucl. Phys. B 966 (2020)

Model	ζ_d	ζ_u	ζ_l
Type I	$\cot\beta$	$\cot\beta$	$\cot\beta$
Type II	$-\tan\beta$	$\cot\beta$	$-\tan\beta$
Type X	$\cot\beta$	$\cot\beta$	$-\tan\beta$
Type Y	$-\tan\beta$	$\cot\beta$	$\cot\beta$
Inert	0	0	0

Current

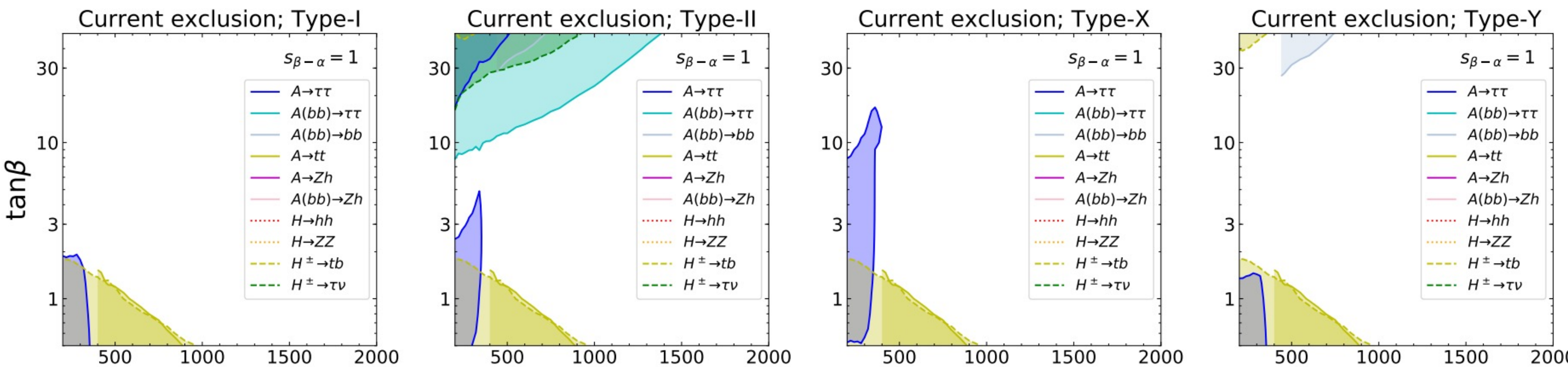

$$H_{2,3} \to \tau\tau$$
$$H_{2,3} \to tt$$
$$H^{\pm} \to tb$$

HL-LHC

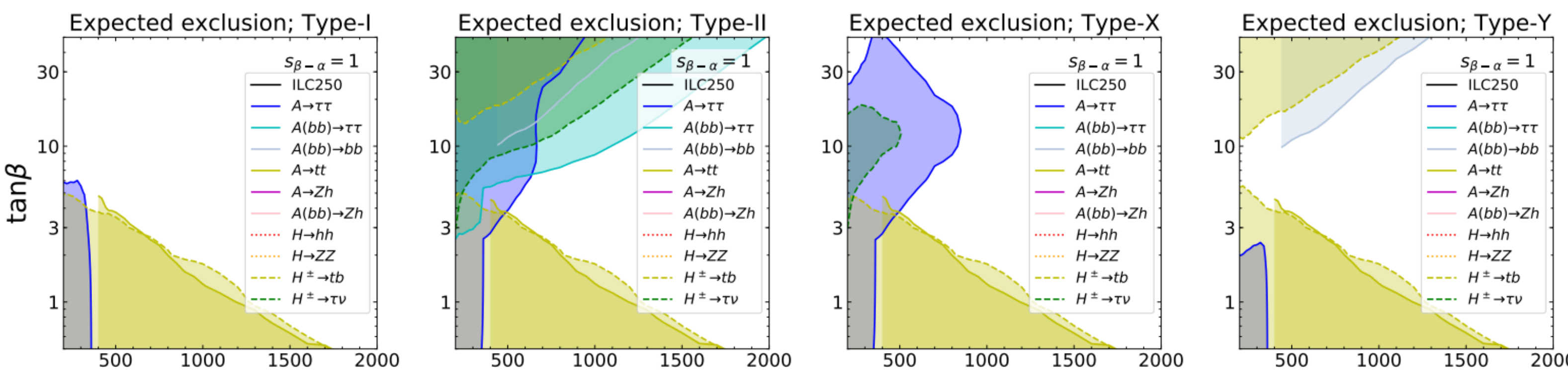

Multi lepton search

Kanemura, Takeuchi and Yagyu, Phys. Rev. D 105 (2022)

$\zeta_u = 0.1$ case

Orange: $B \to X_s + \gamma$
Magenta: $B_s \to \mu\mu$
Cyan: leptonic tau decay
Black shaded: $H \to \tau\tau$
Black curves: multi lepton search

330 GeV

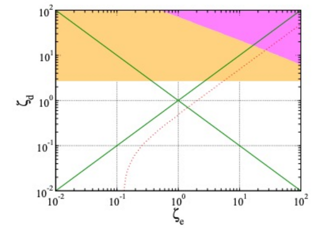

280 GeV

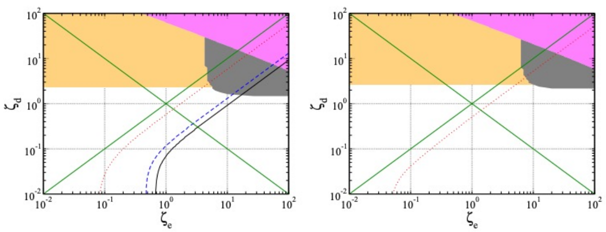

230 GeV

m_{H_2} = 180 GeV

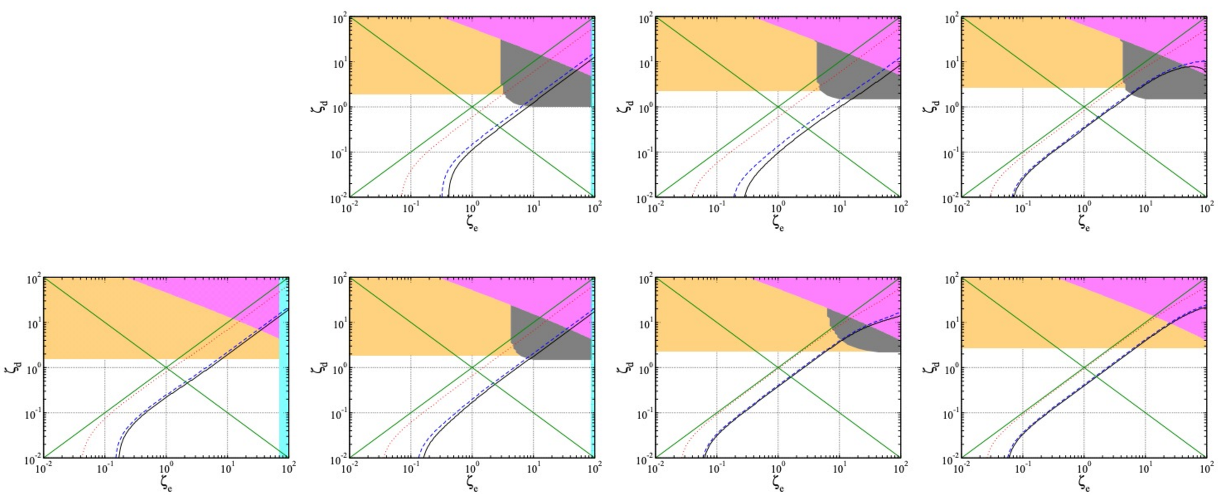

$m_{H_3} = m_{H^\pm}$ = 180 GeV   230 GeV   280 GeV   330 GeV

Other constraints

STU parameter

Considering Higgs alignment and $m_{H_3} = m_{H^\pm}$, our potential has custordial symmetry at 1 loop level.

$$V = -\frac{1}{2}\mu_1^2 \mathrm{Tr}(M_1^\dagger M_1) - \frac{1}{2}\mu_2^2 \mathrm{Tr}(M_2^\dagger M_2) - \mu_{3R}^2 \mathrm{Tr}(M_1^\dagger M_2) + \mu_{3I}^2 \mathrm{Tr}(M_1^\dagger M_2 \tau_3)$$
$$+ \frac{1}{8}\lambda_1 \mathrm{Tr}^2(M_1^\dagger M_1) + \frac{1}{8}\lambda_2 \mathrm{Tr}^2(M_2^\dagger M_2) + \frac{1}{4}\lambda_3 \mathrm{Tr}(M_1^\dagger M_1)\mathrm{Tr}(M_2^\dagger M_2)$$
$$+ \frac{1}{2}\lambda_{5R}\mathrm{Tr}^2(M_1^\dagger M_2) + \frac{1}{4}(\lambda_4 - \lambda_{5R})\left(\mathrm{Tr}^2(M_1^\dagger M_2) - \mathrm{Tr}^2(M_1^\dagger M_2 \tau_3)\right) + \frac{1}{2}\lambda_{5I}\mathrm{Tr}(M_1^\dagger M_2)\mathrm{Tr}(M_1^\dagger M_2\tau_3)$$
$$+ \lambda_{6R}\mathrm{Tr}(M_1^\dagger M_1)\mathrm{Tr}(M_1^\dagger M_2) + \lambda_{6I}\mathrm{Tr}(M_1^\dagger M_1)\mathrm{Tr}(M_1^\dagger M_2\tau_3)$$
$$+ \lambda_{7R}\mathrm{Tr}(M_2^\dagger M_2)\mathrm{Tr}(M_1^\dagger M_2) + \lambda_{7I}\mathrm{Tr}(M_2^\dagger M_2)\mathrm{Tr}(M_1^\dagger M_2\tau_3)$$

Pomarol and Vega, Nucl. Phys. B 413 (1994)

→ T = 0

S and U parameter in general CPV 2HDM Haber and Neil, Phys. Rev. D 83 (2011)

→ S and U are very small in our benchmark scenario.

Bounded from below

Ferreira, Santos and Barroso, Phys. Lett. B 603 (2004)

$$\lambda_1 \geq 0, \quad \lambda_2 \geq 0$$
$$\lambda_3 \geq -\sqrt{\lambda_1\lambda_2}, \quad \lambda_3 + \lambda_4 \mp \lambda_{5R} \geq -\sqrt{\lambda_1\lambda_2}$$
$$|\lambda_{7R}| \leq \frac{1}{4}(\lambda_1 + \lambda_2) + \frac{1}{2}(\lambda_3 + \lambda_4 + \lambda_{5R})$$
$$|\lambda_{7I}| \leq \frac{1}{4}(\lambda_1 + \lambda_2) + \frac{1}{2}(\lambda_3 + \lambda_4 - \lambda_{5R})$$

Unitarity bound (M = 30 GeV) Kanemura and Yagyu, Phys. Lett. B 751 (2015)

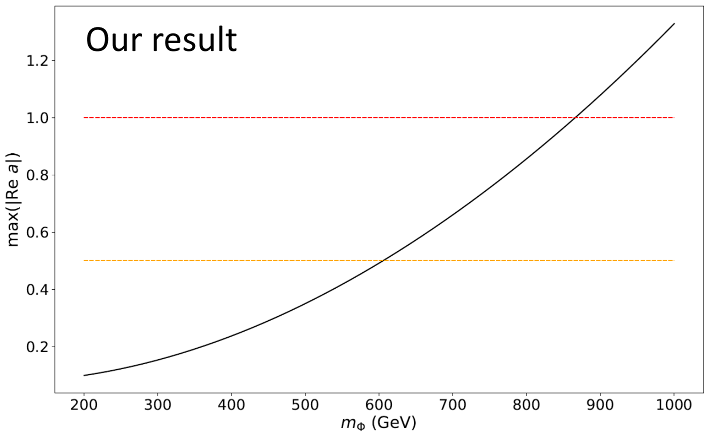

Shape of the chemical potential

When the top transport scenario, θ_7 and θ_u are important for the BAU.

Localized mass around the wall

$$m_t(z) = \frac{y_t}{\sqrt{2}} v(z) e^{i\theta(z)}$$

makes chemical potential.

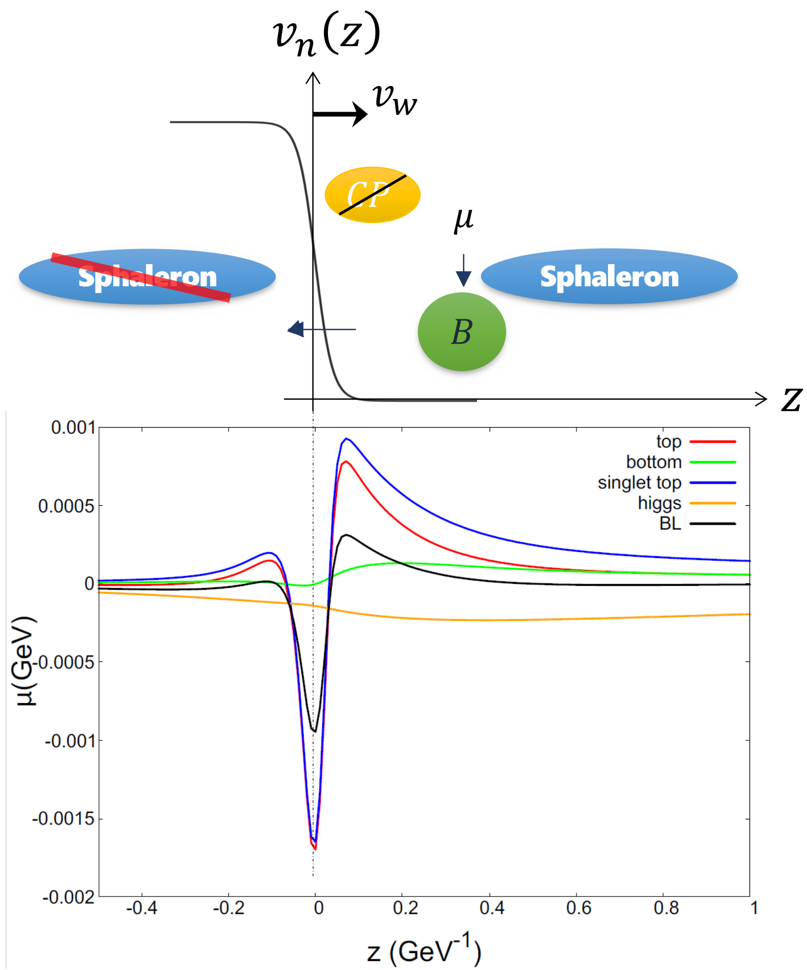

$v(z), \theta(z), T_n,$ etc.
depend on models and dynamics of PT.

About Landau pole

EWPT and triviality bound

- Effective potential with high T expansion

$$V_{eff}(\varphi, T) = D(T^2 - T_0^2) - ET|\varphi|^3 + \frac{\lambda_T}{4}\varphi^4$$

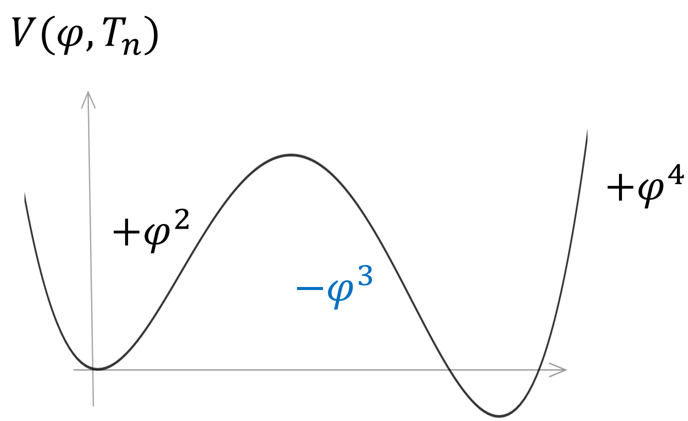

- Non-decoupling effect of heavy scalars

Ex) Two Higgs Doublet Model (2HDM)

$$m_\Phi^2 = M^2 + \tilde{\lambda}v^2 \simeq \tilde{\lambda}v^2 \quad (\tilde{\lambda}v^2 \gg M^2)$$

$$E \simeq \frac{1}{4\pi v^3}\left(m_W^3 + m_Z^3 + m_\Phi^3\right) \sim g^{3/2} + \tilde{\lambda}^{3/2}$$

- Large scalar self couplings are needed for strongly first order PT.

From RGE analysis, Landau pole appears around 1-100 TeV.

Triviality bound : $\Lambda \lesssim 3$ TeV

Cline, Kainulainen and Trott (2011); Kanemura, Senaha and Shindou (2011);
Kanemura, Senaha, Shindou and Yamada (2013); Dorsch, Huber, Konstandin and No (2017); and more

Beyond Landau pole

A new theory is needed above Landau pole.

Ex) Minimal SUSY fat Higgs model Harnik, Kribs, Larson and Murayama (2004)

At the high scale above Landau pole,
scalar couplings behave as non-Abelian gauge couplings

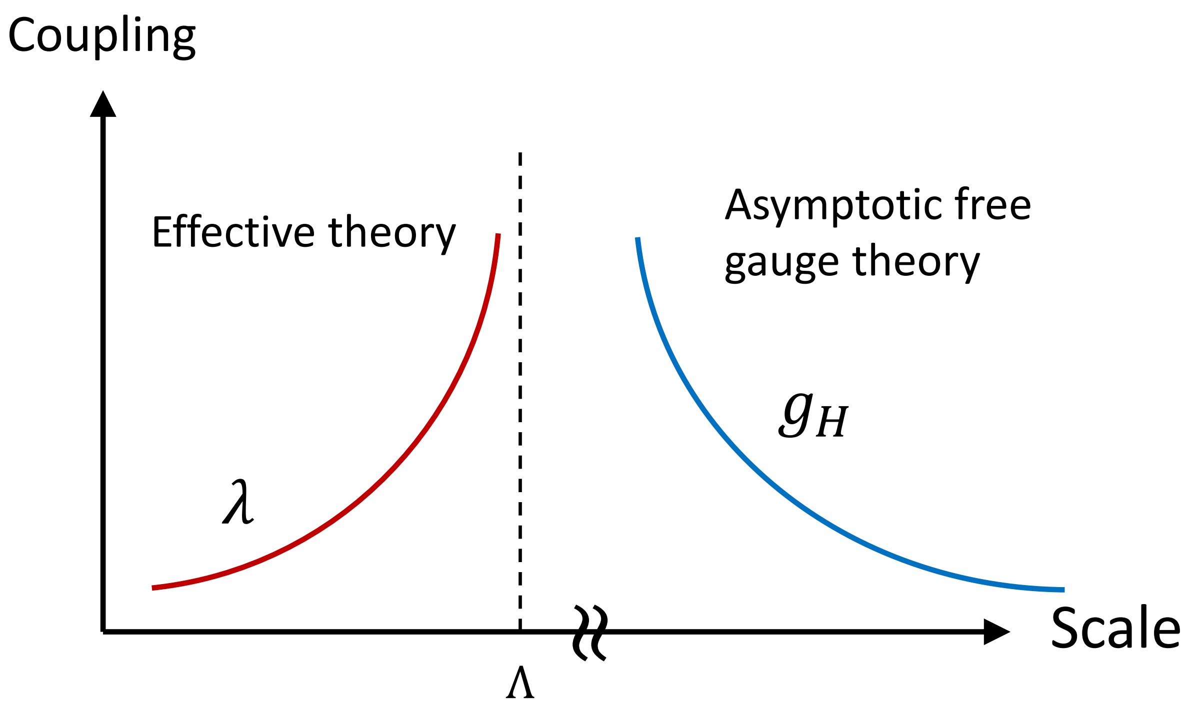

Scalar bosons are meson states as a result of confinement like QCD.

Kanemura, Senaha and Shindou (2011)

RGE analysis

- Scalar self couplings in aligned 2HDM

$$\lambda_1, \lambda_2, \lambda_3, \lambda_4, \lambda_5$$
$$\mathrm{Re}[\lambda_6], \mathrm{Im}[\lambda_6], \mathrm{Re}[\lambda_7], \mathrm{Im}[\lambda_7]$$

- Beta function with dim. reg + $\overline{\mathrm{MS}}$ scheme
(at 1 loop level)
  - Consider threshold effect
Dorsch, Huber, Konstandin and No (2017)

From SM beta function to a2HDM beta function

  - At matching scale,

$$\lambda_i^{\mathrm{SM}}(\tilde{\mu}) = \lambda_i^{\mathrm{A2HDM}}(\tilde{\mu}) \quad (i = 1 \ldots 7)$$
$$\tilde{\mu} = \max\{m_{H_2}, m_{H^\pm}\}$$

No threshold effect
⇒ Landau pole appears around 1-3 TeV (2HDM)

Cline, Kainulainen and Trott (2011)

Scale dependences of couplings (BP1)

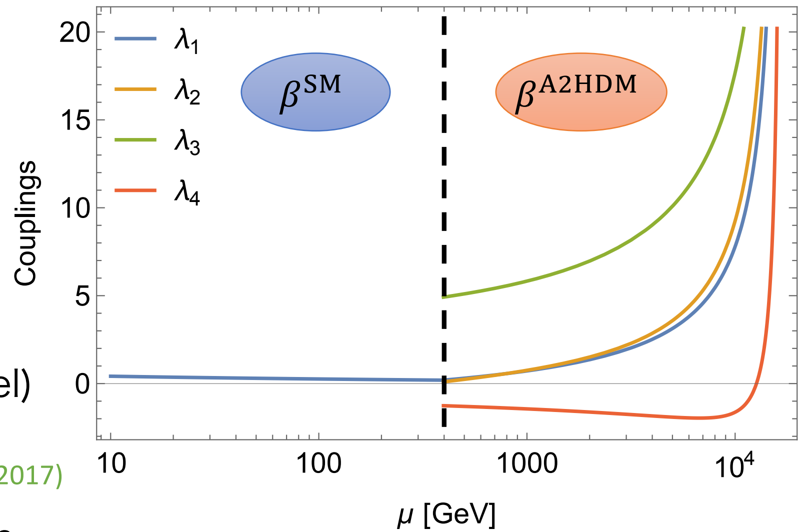

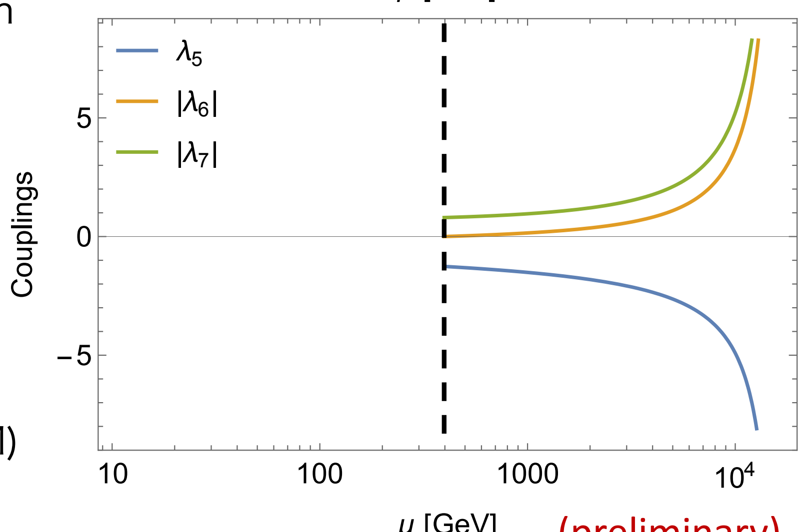

(preliminary)

RGE analysis

- Self-couplings become non-perturbative at $\Lambda_{4\pi}$.

$$\max\{\lambda_i\} > 4\pi \quad (i = 1 \ldots 7)$$

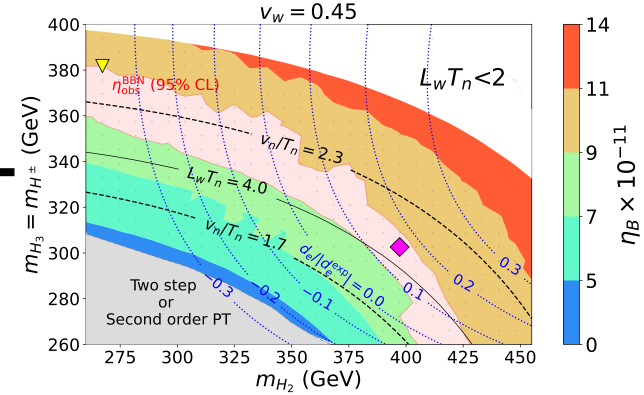

- Strength of PT and v_n/T_n

▽ BP1

$m_{H_2} = 267$ GeV

$m_{H_3} = m_{H^\pm} = 381$ GeV

$M = 30$ GeV

$\Lambda_{4\pi} = 6.7$ TeV

◇ BP2

$m_{H_2} = 397$ GeV

$m_{H_3} = m_{H^\pm} = 302$ GeV

$M = 30$ GeV

$\Lambda_{4\pi} = 13.4$ TeV

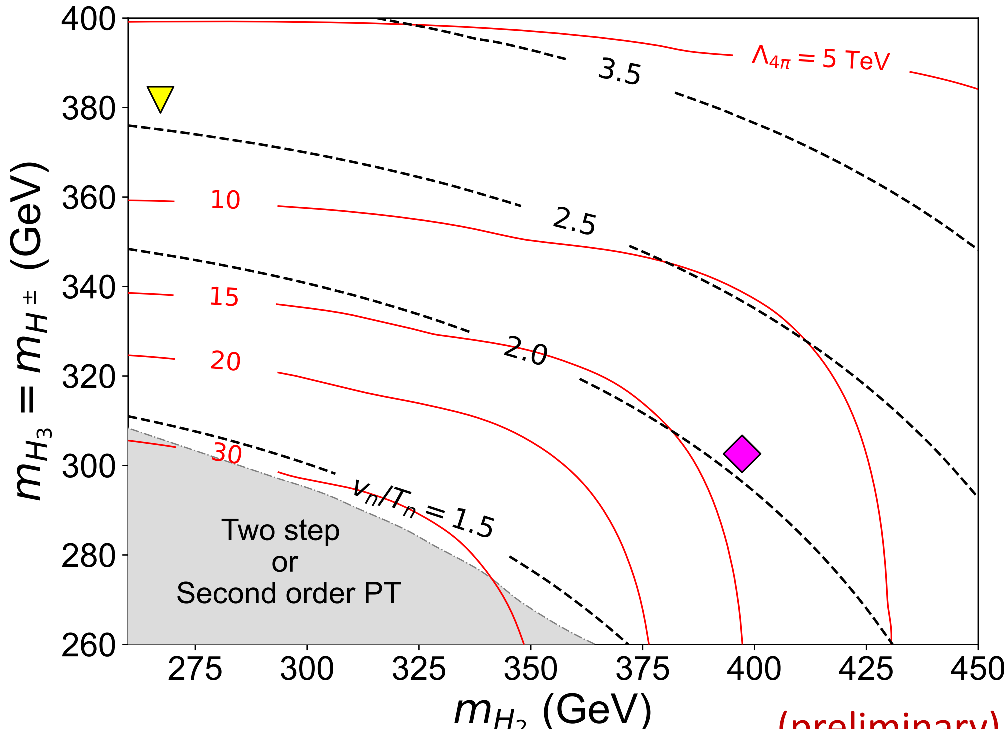

(preliminary)

▽ BP1: Strong PT

◇ BP2: Weak PT

- Benchmark points for GW signal

Landau pole appear around $\Lambda_{4\pi} = O(10)$ TeV